NASA/TP-20230004061

High-Pressure, Normal-Gravity Droplet Combustion Experimental Hardware

Timothy S. Krause
Universities Space Research Association, Glenn Research Center, Cleveland, Ohio

Vittorio M. Valletta
Glenn Research Center, Cleveland, Ohio

Anthony L. Ogorzaly
HX5 Sierra, Cleveland, Ohio

Jay Owens and Daniel J. Gotti
Universities Space Research Association, Glenn Research Center, Cleveland, Ohio

Eric S. Neumann
Glenn Research Center, Cleveland, Ohio

August 2023

NASA STI Program . . . in Profile

Since its founding, NASA has been dedicated to the advancement of aeronautics and space science. The NASA Scientific and Technical Information (STI) Program plays a key part in helping NASA maintain this important role.

The NASA STI Program operates under the auspices of the Agency Chief Information Officer. It collects, organizes, provides for archiving, and disseminates NASA's STI. The NASA STI Program provides access to the NASA Technical Report Server—Registered (NTRS Reg) and NASA Technical Report Server—Public (NTRS) thus providing one of the largest collections of aeronautical and space science STI in the world. Results are published in both non-NASA channels and by NASA in the NASA STI Report Series, which includes the following report types:

- TECHNICAL PUBLICATION. Reports of completed research or a major significant phase of research that present the results of NASA programs and include extensive data or theoretical analysis. Includes compilations of significant scientific and technical data and information deemed to be of continuing reference value. NASA counter-part of peer-reviewed formal professional papers, but has less stringent limitations on manuscript length and extent of graphic presentations.

- TECHNICAL MEMORANDUM. Scientific and technical findings that are preliminary or of specialized interest, e.g., "quick-release" reports, working papers, and bibliographies that contain minimal annotation. Does not contain extensive analysis.

- CONTRACTOR REPORT. Scientific and technical findings by NASA-sponsored contractors and grantees.

- CONFERENCE PUBLICATION. Collected papers from scientific and technical conferences, symposia, seminars, or other meetings sponsored or co-sponsored by NASA.

- SPECIAL PUBLICATION. Scientific, technical, or historical information from NASA programs, projects, and missions, often concerned with subjects having substantial public interest.

- TECHNICAL TRANSLATION. English-language translations of foreign scientific and technical material pertinent to NASA's mission.

For more information about the NASA STI program, see the following:

- Access the NASA STI program home page at http://www.sti.nasa.gov

- E-mail your question to help@sti.nasa.gov

- Fax your question to the NASA STI Information Desk at 757-864-6500

- Telephone the NASA STI Information Desk at 757-864-9658

- Write to:
  NASA STI Program
  Mail Stop 148
  NASA Langley Research Center
  Hampton, VA 23681-2199

NASA/TP-20230004061

High-Pressure, Normal-Gravity Droplet Combustion Experimental Hardware

Timothy S. Krause
Universities Space Research Association, Glenn Research Center, Cleveland, Ohio

Vittorio M. Valletta
Glenn Research Center, Cleveland, Ohio

Anthony L. Ogorzaly
HX5 Sierra, Cleveland, Ohio

Jay Owens and Daniel J. Gotti
Universities Space Research Association, Glenn Research Center, Cleveland, Ohio

Eric S. Neumann
Glenn Research Center, Cleveland, Ohio

National Aeronautics and
Space Administration

Glenn Research Center
Cleveland, Ohio 44135

August 2023

Acknowledgments

The authors would like to gratefully acknowledge the feedback of Vedha Nayagam and Daniel Dietrich throughout the design process and implementation of the experimental hardware configuration.

This report contains preliminary findings, subject to revision as analysis proceeds.

Level of Review: This material has been technically reviewed by expert reviewer(s).

This report is available in electronic form at https://www.sti.nasa.gov/ and https://ntrs.nasa.gov/

Contents

High-Pressure, Normal-Gravity Droplet Combustion Experimental Hardware

Timothy S. Krause
Universities Space Research Association
Glenn Research Center
Cleveland, Ohio 44135

Vittorio M. Valletta
National Aeronautics and Space Administration
Glenn Research Center
Cleveland, Ohio 44135

Anthony L. Ogorzaly
HX5 Sierra
Cleveland, Ohio 44135

Jay Owens and Daniel J. Gotti
Universities Space Research Association
Glenn Research Center
Cleveland, Ohio 44135

Eric S. Neumann
National Aeronautics and Space Administration
Glenn Research Center
Cleveland, Ohio 44135

Summary

The High-Pressure, Trans-Critical (HPTC) 1-g Liquid Droplet Combustion Experiments will assess the autoignition and combustion of liquid fuel droplets at elevated temperatures and pressures. These experiments are being conducted at the NASA Glenn Research Center in a manner similar to experiments performed in Glenn's Zero Gravity Research Facility (ZGF) using the B drop vehicle. The modification to the test capabilities of the ZGF experiments in the new experimental configuration will allow researchers to continue performing normal-gravity liquid droplet combustion experiments without requiring the use of the ZGF test equipment.

These normal-gravity experiments will be conducted at lower pressures than in the ZGF because the pressure vessel for this setup is limited to a maximum working pressure of 7.74 atm (99.1 psig) at 366.5 K (200 °F). This experimental configuration will enable development of a similar capability for conducting high-pressure combustion and supercritical oxidation research on the International Space Station. Experiments will be conducted with the capability of altering the ambient pressure, temperature, and gas concentrations, as well as the fuel type for each test. For these experiments, the test vessel operates at pressures up to 7.5 atm (95.5 psig), temperatures up to 1,073 K (1,472 °F) inside the insulated oven, and oxygen concentrations up to 30 percent.

1.0 Introduction

The testing apparatus (Figure 1) consists of a pressure vessel, an insulated oven, a video data acquisition (VDAQ) system, and temperature and pressure measurement devices. The pressure vessel has two sections: a lower, unheated section for droplet deployment and an upper, heated section is where autoignition and combustion occur. A single liquid fuel droplet, approximately 1 mm (0.039 in.) in diameter, is dispensed from a high-pressure syringe pump through a small-diameter tubing system onto the end of a quartz fiber.

Once deployed, the droplet and fiber are translated upward into the oven on a cart controlled by a stepper motor. The translation of the droplet into the oven is synchronized with the triggering of the high-speed data acquisition and video imaging systems. Once inside the heated zone, the droplet is exposed to the elevated temperature and pressure conditions, and autoignition should ensue quickly under these conditions. The ignition and combustion of the droplet are recorded by two video imaging systems; a data acquisition system simultaneously records the temperature and

pressure data. The translation and combustion of the droplet take less than 10 s. A simplified schematic of the experimental setup is shown in Figure 2.

2.0 Mechanical Components

2.1 Pressure Vessel

The experiments are performed inside an aluminum pressure vessel machined from a single billet of aluminum. Several of these chambers were manufactured more than a decade ago for the microgravity combustion science program. Although the chambers were designed with the intent of meeting the American Society of Mechanical Engineers (ASME) code, they are not code stamped. The vessel has an internal volume of approximately 15,400 cm^3 (942 in^3) and is rated for 7.74 atm (99.1 psig) at 366.5 K (200 °F). Four orthogonal 25.4-mm- (1-in.-) thick rectangular quartz windows allow imaging the droplet deployment and droplet combustion event. Engineering drawings of the pressure vessel are shown in Figure B.1 to Figure B.4 in Appendix B.

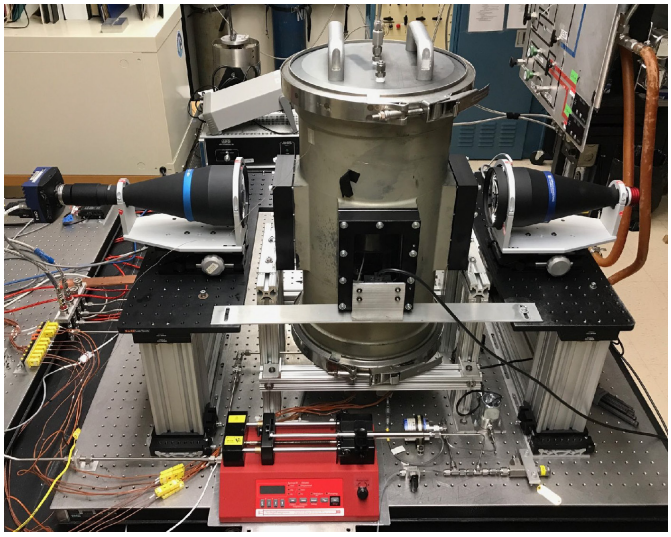

Figure 1.—HPTC experimental setup.

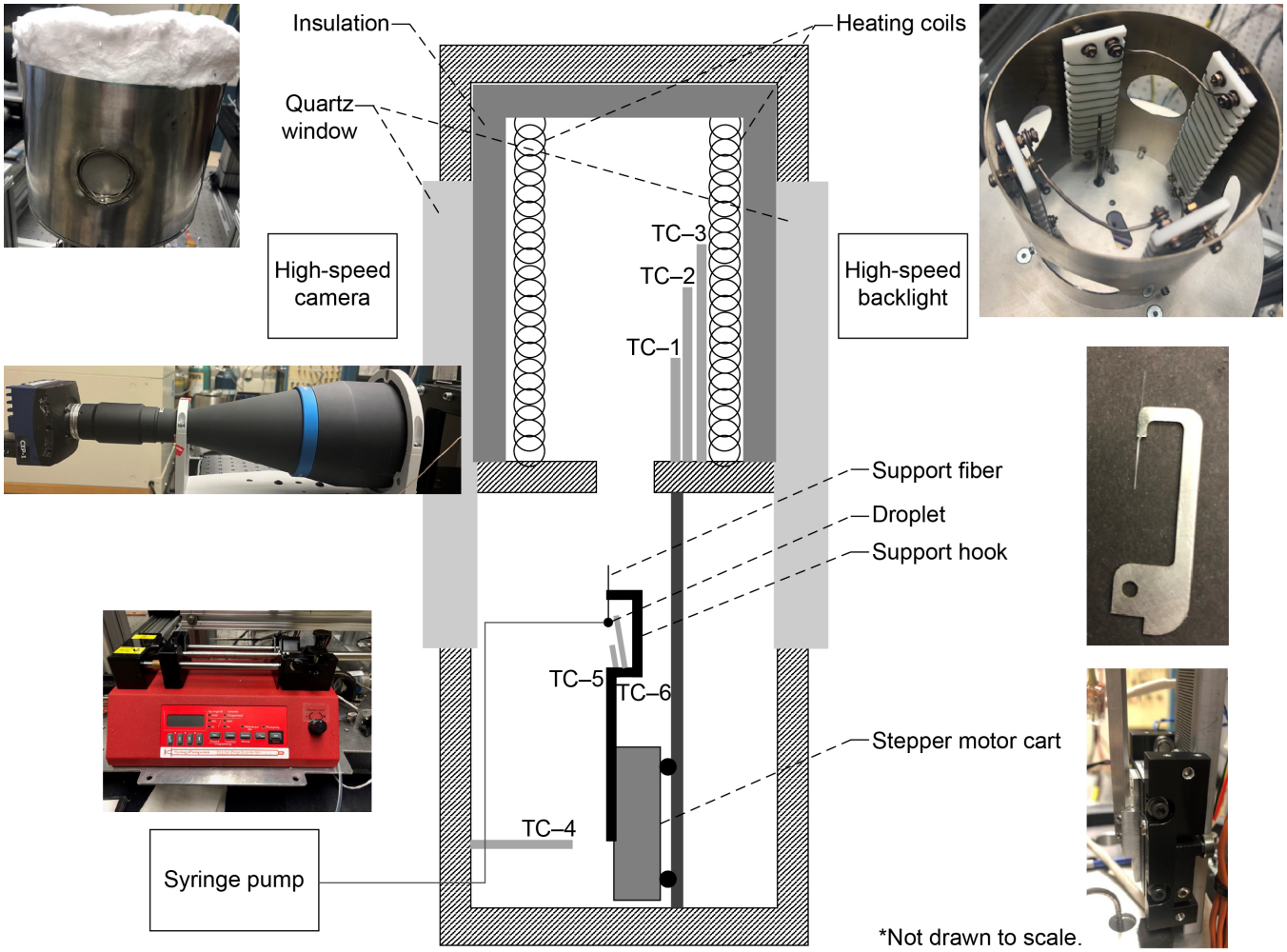

Figure 2.—Schematic of HPTC experimental setup.

2.2 Heater Oven

A custom resistance heater oven, designed for internal temperatures of up to 1,073 K (1,472 °F), is located inside the top half of the vessel. The total area of heated volume is approximately 786.5 cm^3 (48 in^3). Four 31.75-mm- (1.25-in.-) round sapphire windows allow imaging the combustion event. Figure B.5 to Figure B.9 illustrate the heaters and heater housing. The heaters are insulated with 25.4-mm (1-in.) Cerablanket® RCF–24 703024 refractory fiber insulation (Morgan Advanced Materials), which has a thermal conductivity of 0.06 W/mK at 573 K (500 °F).

2.3 Fiber and Hook

A single liquid droplet is deployed onto a 125-μm (0.005-in.) quartz fiber in the unheated region of the vessel. The fiber holds a 275- to 300-μm (0.011- to 0.012-in.) bead on its end. The bead's diameter varies slightly because it is made by melting the end of the quartz to ensure the fiber is made up of all the same material. The thermal conductivity of the fiber is approximately 1.1 W/mK. The fiber is attached to the stepper motor by a three-piece stainless steel assembly (Figure B.10 to Figure B.12). The fiber is glued to a support hook, which screws into a post so that it is positioned at a 45° angle with respect to both the color camera and the high-speed camera. The post is then secured to the stepper motor cart via a small bracket.

2.4 Stepper Motor

Once a droplet has been deployed, the cart can be translated, which moves the droplet and quartz fiber into the oven, exposing the droplet to the high temperature. This cart is driven by a built-in 8.9-N (2-lb) continuous-force stepper motor (H2W Technologies LMSS0602–2WW0), which uses roller bearing supports. The inserted droplet takes 420 ms to travel 64.5 mm (2.54 in.) and follows an S-shaped displacement trajectory at 250 pulse/mm (6,350 pulse/in.), as shown in Figure B.13. The insertion is controlled by a stepper motor driver (Automation Direct STP–DRV–4850) and is synchronized to 2 s after the start of data acquisition.

2.5 Pressure Control

Three independent pressure systems feed the test cell, controlling both the ambient test cell pressure and the pressure in the fuel supply line. Figure 3 is a schematic of the pressure systems. Figure B.14 in Appendix B provides a more detailed flow diagram with part numbers. Part numbers and pressure and temperature ratings of all components are listed in Table B.1.

The pressure is controlled by a back pressure regulator; the pressure at various points in the system is relayed back to the user through the user interface, as shown in Figure 4. The user interface also allows for control of the pressure at various points through manual and solenoid-actuated valves. These valves allow for control of venting upon test completion, as well as allowing the dispersal of fuel onto the fiber during the deployment stage.

2.5.1 Gas Pressure Control

The first pressure system is the air/oxidizer system, which supplies the atmosphere to the test cell. The chamber fill system is connected through the laboratory air/inert supply system (TCC–0110–R218–INERT) to a K bottle of premixed gas with the desired concentrations of oxygen and diluents. The second pressure system pressurizes the dome of a dome-loaded back pressure regulator to precisely maintain the desired pressure in the test chamber as its atmosphere is heated. The pressure for the vessel pressure control system is supplied via a second K bottle filled with zero air in the laboratory system. The test vessel is protected by an ASME relief valve set at 7.8 atm (100 psig); both K bottles have 11.2-atm (150-psig) relief valves installed immediately downstream from the cylinder regulators.

2.5.2 Fuel Pressure Control

The third pressure system provides the liquid fuel to the test cell. A high-pressure syringe pump (New Era NE–8000X2) is used to deploy the liquid droplet onto the fiber. The pump has an 8-ml (0.27-oz) stainless steel syringe (KD Scientific 780807) attached to control the fuel flow. A 14.6-atm (200-psig) relief valve protects the fuel system from overpressurization. A solenoid actuator at the end of the fuel line allows for horizontal translation of the needle for deployment onto the fiber.

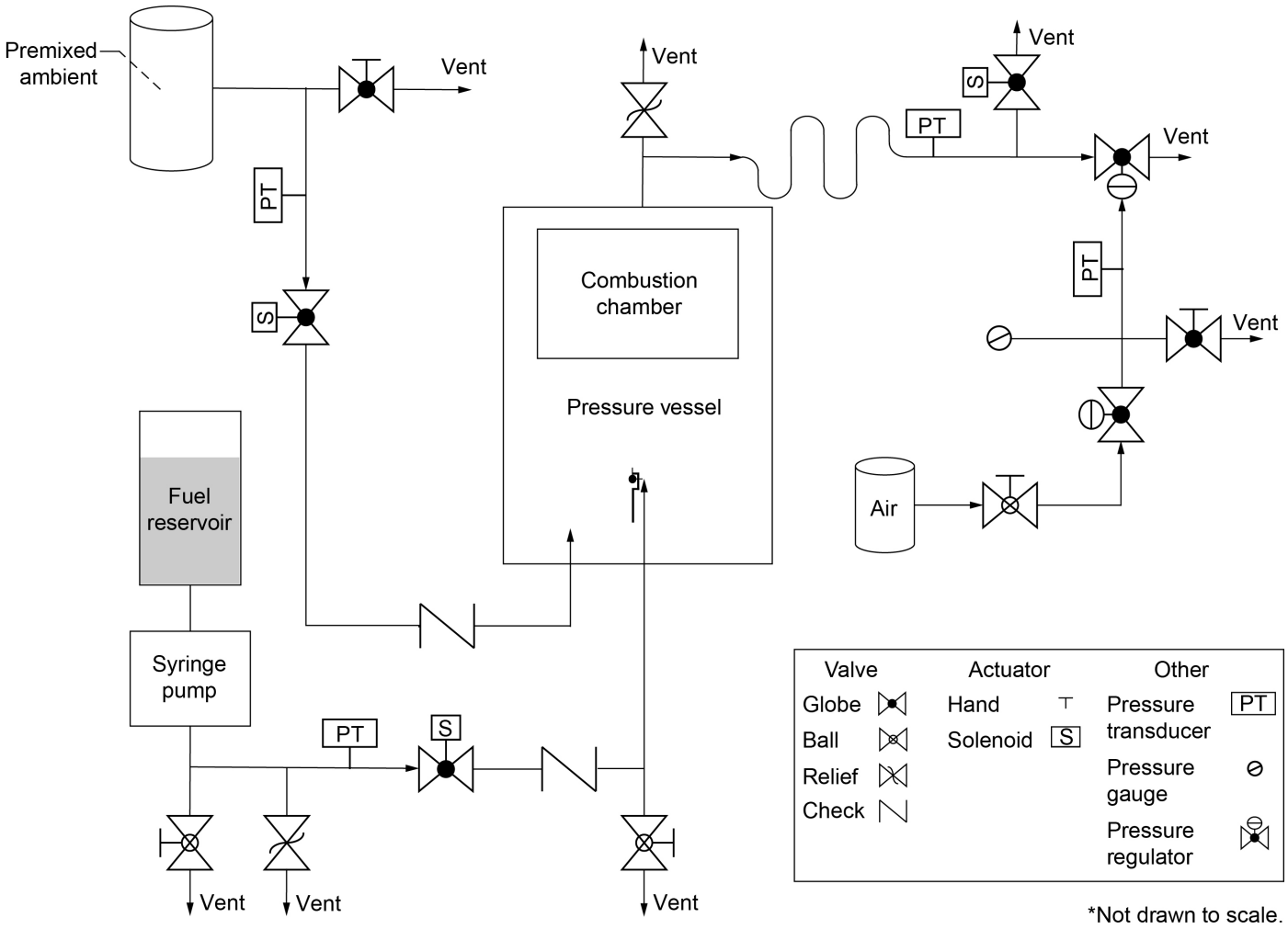

Figure 3.—Three pressure systems that feed test cell.

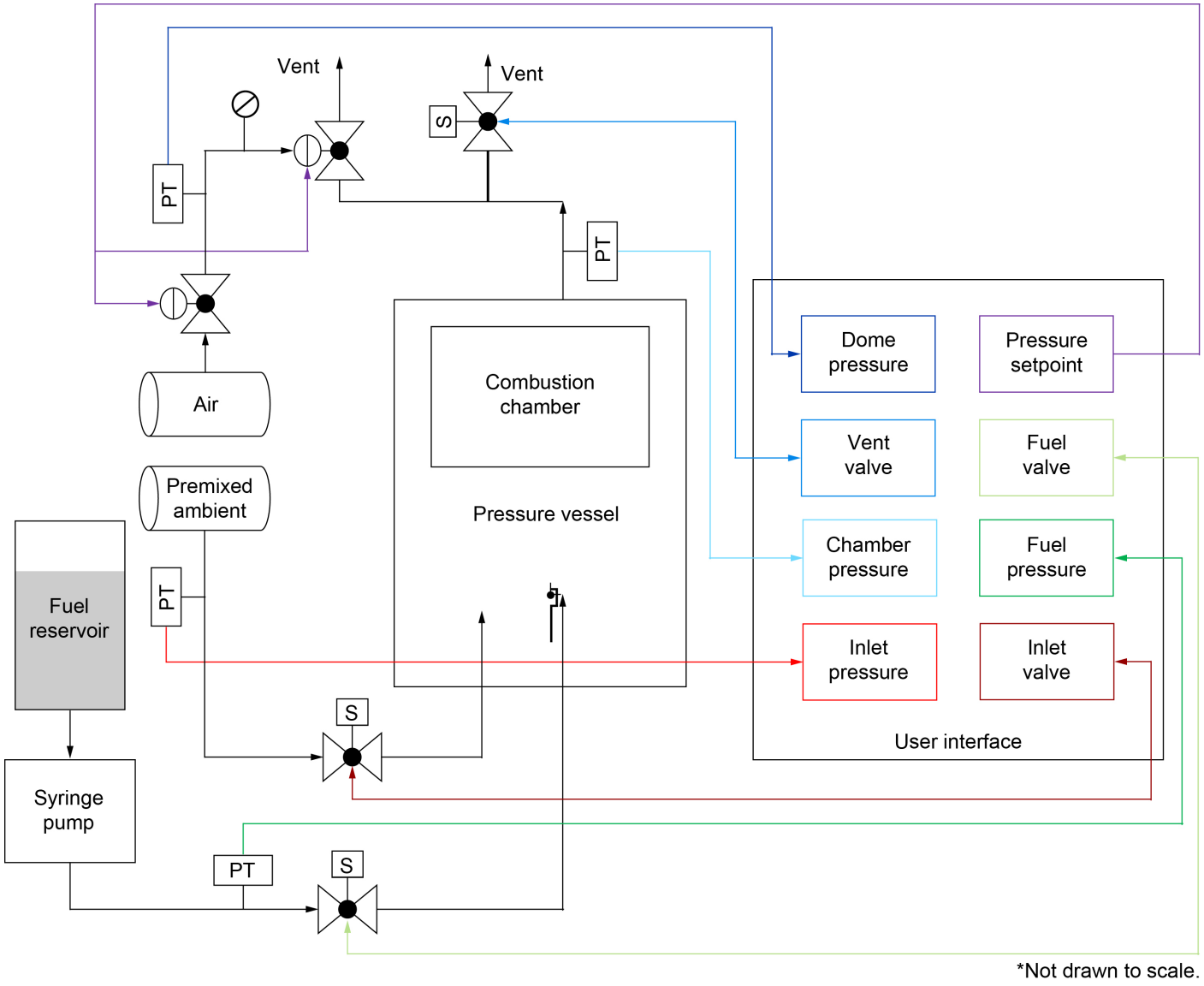

Figure 4.—Three pressure systems that feed test cell with user interface.

2.6 Temperature Control

Seven Type K thermocouples (Omega Engineering, Inc.) are located inside the chamber. One surface-temperature thermocouple (TC–7) is attached to the wall of the upper, heated zone of the test vessel to provide vessel temperature feedback to the operator and automated shutdown of the resistance heaters if the vessel wall temperature approaches the vessel temperature limit of 366.5 K (200 °F). A second exposed-tip thermocouple (TC–4) sits in the lower, unheated portion of the chamber, 11 cm (4.33 in.) below the entrance of the oven, to provide the ambient temperature of the lower chamber. An additional grouping of three sheathed, ungrounded-tip thermocouples (TC–1 to TC–3) is positioned in the heated region as a thermocouple rake. The lowest (TC–1) and highest (TC–3) thermocouples in the rake are located 42 mm (1.65 in.) and 71 mm (2.80 in.) above the entrance to the oven, respectively. The center thermocouple of the rake (TC–2) provides feedback to the user on the heated region temperature and is located at 64.5 mm (2.54 in.), the same vertical height as the droplet position. All rake thermocouples are located 24.8 mm (0.976 in.) radially from the center of the chamber. Two exposed-tip thermocouples (TC–5 and TC–6) with response times of less than 10 ms are placed in the vicinity of the droplet and attached to the stem of the hook. The quick response time of these thermocouples allows them to be used to verify ignition and temperatures in close proximity to the droplet. Both of these thermocouples are placed 3 mm (0.12 in.) radially from the droplet location. TC–5 is placed 5 mm (0.20 in.) vertically below the droplet and TC–6 is placed 1 mm (0.049 in.) vertically above the droplet. The locations of all the thermocouples and their display on the user interface are shown in Figure 5 and Table I. The temperatures are regulated by a PID temperature controller (Omega Platinum™ CN16Pt–305–EIP–DC) using TC–2 as the setpoint.

TABLE I.—VERTICAL AND RADIAL LOCATION OF THERMOCOUPLES IN CHAMBER

Thermocouple	Vertical location, *z*, mm	Radial location, *r*, mm	Type
TC–1	42	24.8	Ungrounded
TC–2	64.5	24.8	
TC–3	71	24.8	
TC–4	–11	26	Exposed
TC–5	59.5	3	
TC–6	65.5	3	
TC–7	≈220	≈135	Surface

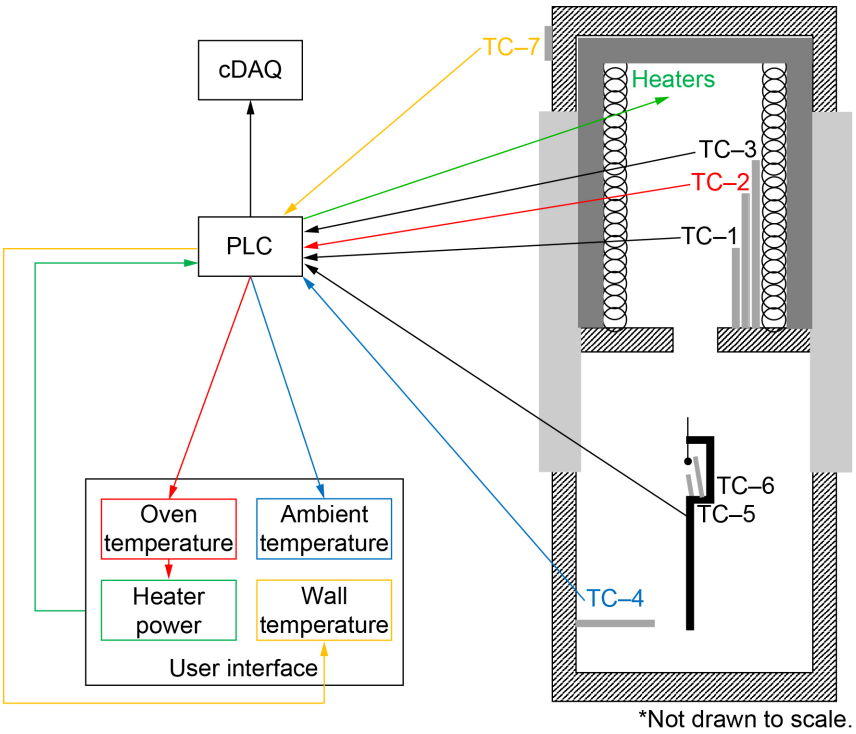

Figure 5.—Temperature connections and user interface.

3.0 Electrical Components

The experimental test setup is powered via a commercial 24-Vdc power supply (Industrial Power Supply P24–150D) and a 110-Vac 60-Hz power supply (Wiremold UL209BC). Alternating current (AC) power is used for the oven heater. The experiment is controlled with a programmable logic controller (PLC) (Direct Logic DO–06DR) (Figure B.15). This PLC controls the timing and initiation of experiment events such as droplet deployment, oven temperature setpoint, droplet translation, and triggering of the data acquisition and video systems. The PLC is interfaced with a touchscreen operator panel that displays a graphical user interface (Figure 6) for experiment operation, as well as critical system temperatures, pressures, and setpoints.

The analog voltage data is recorded on a data logger (National Instruments NI–cDAQ9132 Compact Data Acquisition (cDAQ)). The cDAQ data logger is a 32-channel, differential input, data acquisition system with cold junction temperature compensation for thermocouple inputs. It records all voltage data from the experiment pressure transducers and thermocouples. The data is stored on a compact flash card for posttest retrieval. The sampling rate for the cDAQ is controlled by an application created in the LabVIEW programming environment and set at 1,000 sample/s to correspond with the frame rate of the high-speed camera. Figure 7 is a simplified schematic of the data acquisition triggers and connections. Detailed wiring diagrams for the electrical components are included in Appendix B in Figure B.15 to Figure B.19. Figure 8 is a simplified component connection schematic.

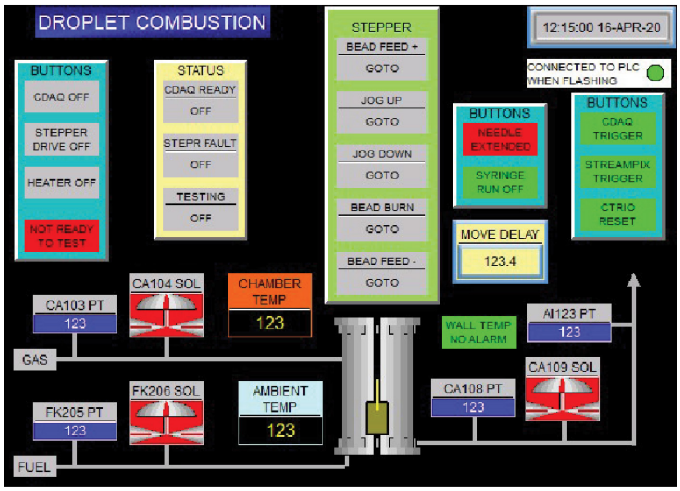

Figure 6.—Touchscreen user interface display provides critical test parameters to operator.

4.0 Optical Components

Three cameras are positioned to capture the test events. Two are placed with a line of sight into the upper chamber to capture the combustion events; the other views the lower portion of the chamber to capture droplet deployment. All camera data are recorded on a local personal computer (PC) running high-speed digital video recording software (NorPix StreamPix). The images are saved in 8-bit .seq format, a NorPix proprietary format that can be converted to an audio video interleave (.avi) or tagged image file format (.tiff) file. The cameras are synchronized via a pulse generator (Berkeley Nucleonics 525) that controls the triggers of all the cameras. The timestamps for all the images correspond to the PC's internal clock. Outputs from the cameras are also displayed on a monitor in view of the operator.

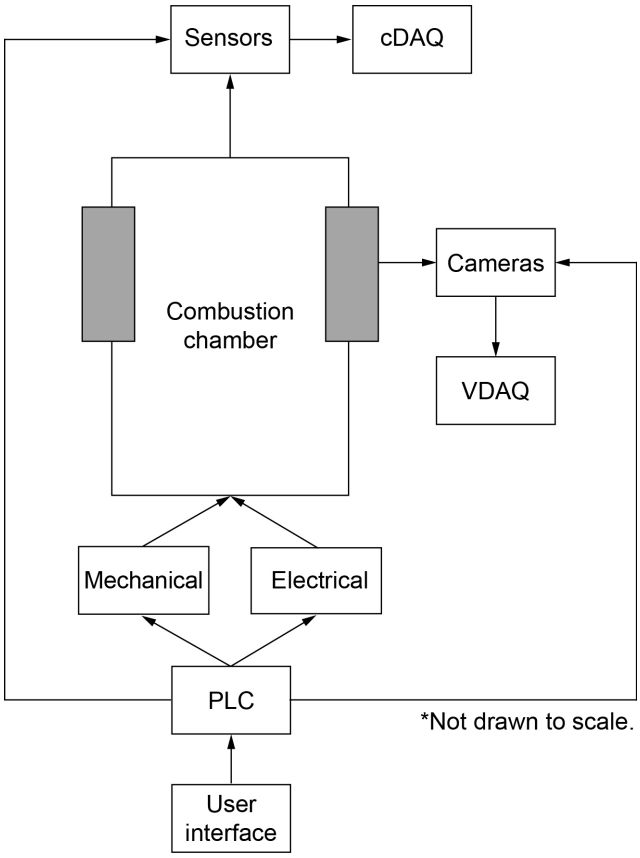

Figure 7.—Data acquisition components and connections.

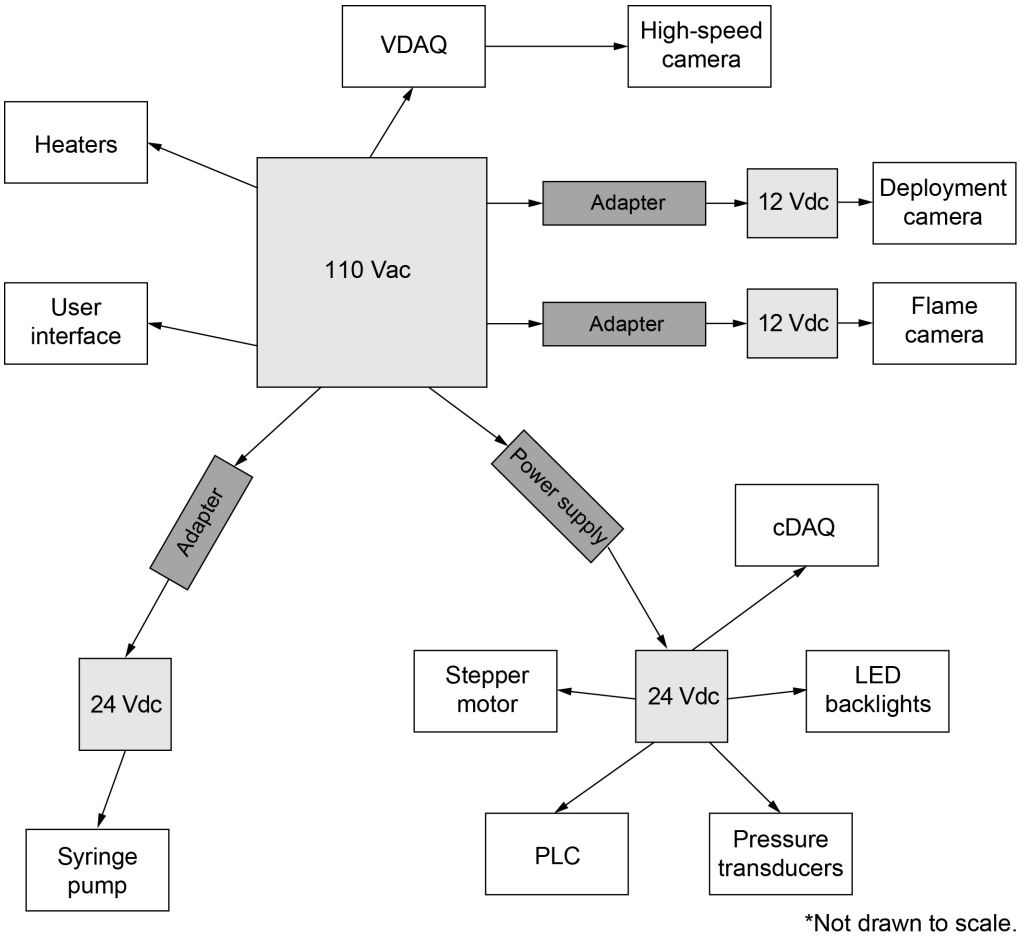

Figure 8.—Electrical components and connections.

4.1 Combustion Cameras

Two cameras are positioned orthogonally outside the upper portion of the chamber to capture the combustion events. The first is a monochrome high-speed camera designed to capture the droplet regression and cool flame propagation; the second is a high-definition (HD) color camera to capture the flame. Figure 9 shows a top view diagram of the cameras.

4.1.1 High-Speed Camera

A digital high-speed monochrome camera (Mikrotron model MC4082) is set up to capture the droplet as a shadowgraph. The camera has a frame rate of 1,000 frames per second (fps) with a resolution of 960×960 pixels. The gain, exposure, and black level are fixed throughout the test at 80 dB, 570 µs, and 0, respectively. The camera is illuminated by a collimated light-emitting diode (LED) backlight (Opto Engineering model LTCLHP080–G) at a wavelength of 525 nm. The backlight is synchronized to the high-speed camera by a controller (Gardasoft model PP420F), which sets the LED power level and pulse duration. For this test setup, the LED power level is 50 percent and strobe duration is set to continuous illumination. The camera is also equipped with a telecentric lens (Opto Engineering model TC4MHR080–C) with an f/16 aperture and a 525-nm bandpass filter (Opto Engineering model FTBP525TC).

4.1.2 Flame Camera

The flame is captured at 180 fps with a USB3 HD color video camera (FLIR GS3–U3–23S6C). The resolution for this camera is 1024×1024 pixels with a variable gain and 5,000-µs exposure. The camera is equipped with a 70-mm lens (Schneider TeleXenar) with a 25-mm extension tube. The lens has an f/2.2 aperture and is prefocused manually on the bead fiber at the center of the flame.

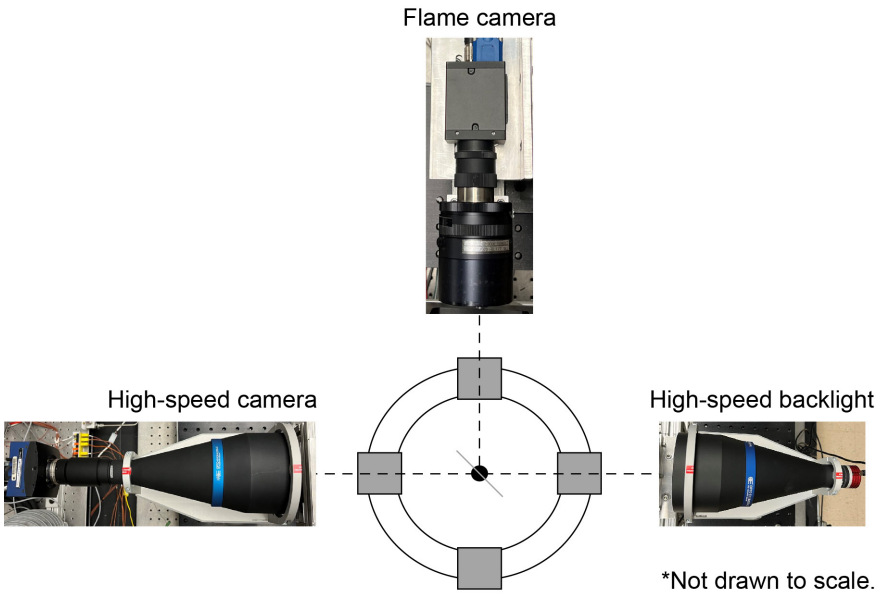

Figure 9.—Top view of combustion cameras and backlight.

4.2 Deployment Camera

A Gigabit Ethernet HD monochrome camera (Allied Vision Prosilica GT 1290) provides the operator with a shadowgraph view of droplet deployment prior to the droplet translation into the combustion chamber. The resolution is set at 960×960 pixels, and video is captured at 30 fps. The exposure of the camera is 25 ms, and the gain is adjusted automatically throughout the test. The camera is fitted with a telecentric lens (Opto Engineering model RT–TV–1M–220) with an f/20 aperture. The continuous illumination is controlled by a collimated LED panel (Advanced Illumination model CB0101–520–24) with a wavelength of 520 nm. Figure 10 is a top view of the camera.

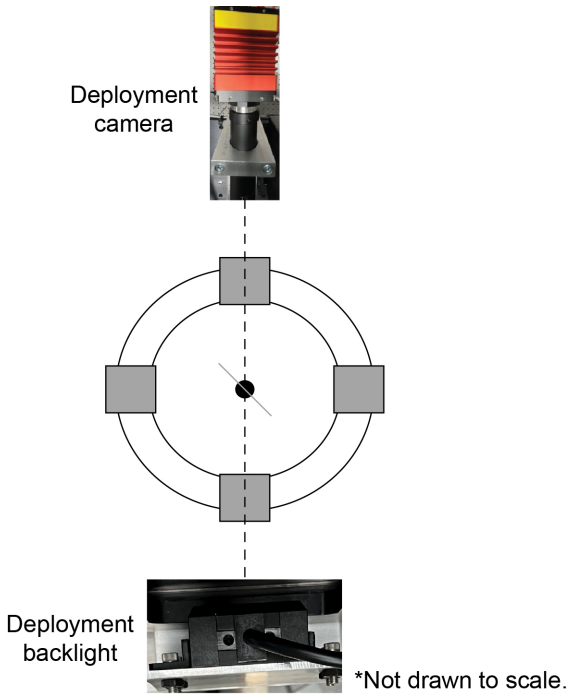

Figure 10.—Top view of deployment camera and backlight.

5.0 Operation

The test vessel is divided into two sections. The lower portion of the vessel, which contains the droplet deployment and translation hardware, is unheated, so it is maintained at a lower temperature. The upper portion of the vessel, where the droplet combustion event occurs, contains a heavily insulated, resistance-heated oven. The chamber is heated to 100 K higher than the desired temperature setpoint and the heaters remain powered for 10 min. After 10 min, the heaters are turned off to allow for a more uniform thermal gradient inside the oven as the temperature decays. As the chamber approaches the desired

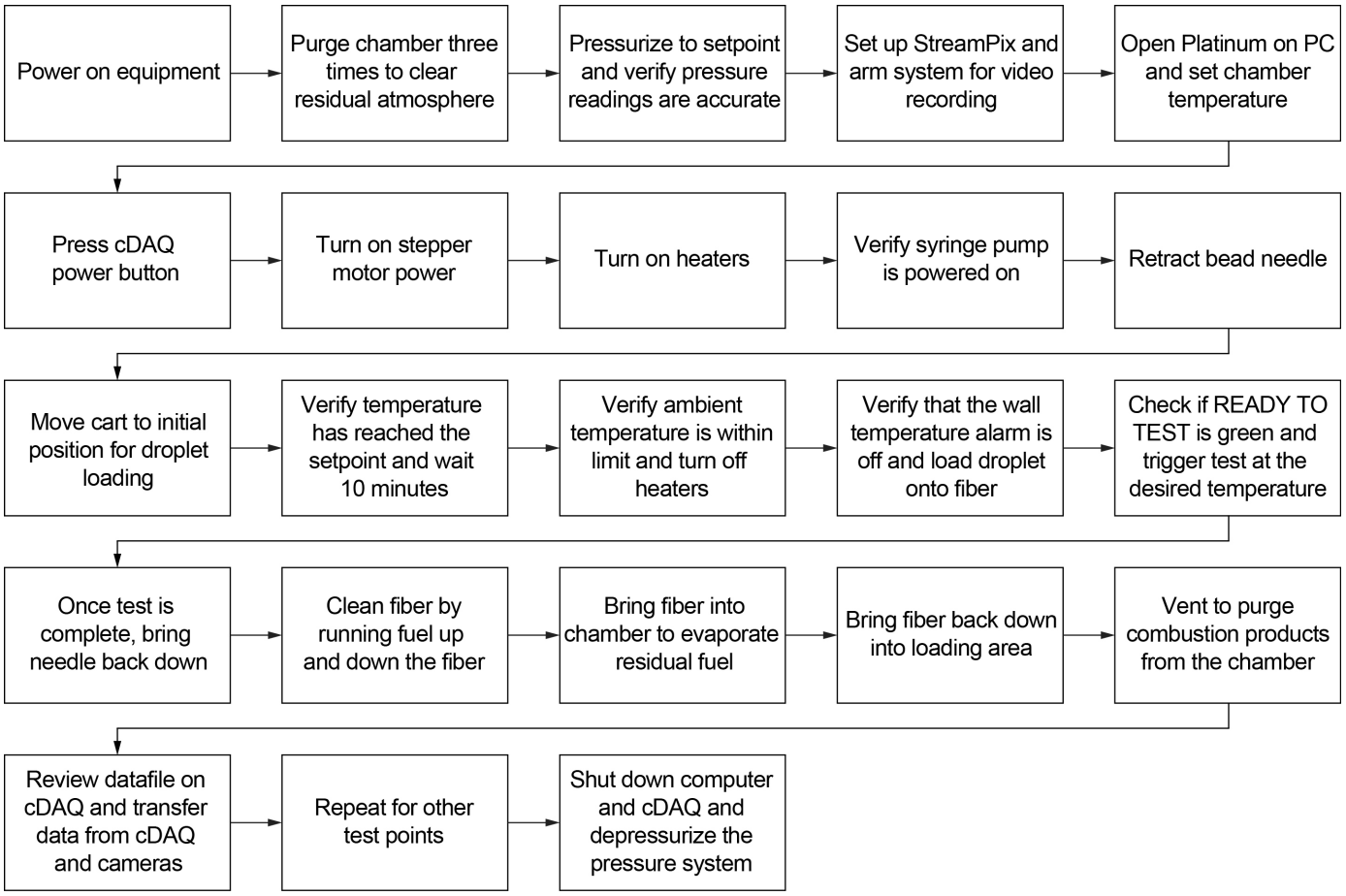

Figure 11.—Experiment operation process flow.

temperature, a single liquid fuel droplet, about 1 mm in diameter, is dispensed from a high-pressure syringe pump through a small-diameter tubing system onto the end of a quartz fiber. Once deployed, the droplet and fiber are translated upward into the oven on a stepper motor-controlled cart. The translation of the droplet into the oven is synchronized with the trigger of the high-speed data acquisition and video imaging systems. Data are acquired for 2 s before insertion and 10 s after insertion. Once in the heated zone, the droplet is exposed to the elevated temperature and pressure conditions, where autoignition should quickly ensue. Multiple tests may be run consecutively until the vessel's temperature limits are reached. Between tests, the chamber is depressurized by opening the vent valve, then repressurized after closing the vent valve. To ensure all residual combustion products have been cleared from the chamber, this process is repeated three or more times. A detailed process flow diagram for the experiment is shown in Figure 11.

6.0 Concluding Remarks

The High-Pressure, Trans-Critical (HPTC) 1-g Liquid Droplet Combustion Experiments will provide researchers with a useful environment for studying the autoignition of various fuels under varying ambient conditions. The experimental configuration allows for variation of pressure up to 7.5 atm (95.5 psig), temperature up to 1,073 K (1,472 °F), and oxygen concentrations up to 30 percent. Various other diluents may also be used in the facility to study the influence of diluents on flame behavior. The quick turnaround time of the apparatus from test to test allows for the rapid progression through test matrices, which can inform test points in the Zero Gravity Research Facility (ZGF) apparatus. This experimental configuration will be used to generate regime maps and autoignition curves for a variety of fuels in different ambient conditions, which provides a unique resource for researchers when studying the autoignition dynamics of various fuels.

Appendix A.—Calibration and Characterization

To ensure the usability of the experimental apparatus, various calibrations and characterizations were run on the rig. The first was scaling the cameras to convert from pixels to millimeters. The second involved optimizing the high-speed gain and exposure settings to ensure maximum visibility of the cool flame. The third was characterizing the stepper motor to ensure the repeatability of the insertion procedure. The fourth involved characterizing the temperature field in the chamber.

A.1 Camera Scaling

The high-speed and color cameras were calibrated using two targets: a grid of 2-mm (0.079-in.) squares and a 1951 U.S. Air Force (USAF) R1L1S1N resolution test chart. The targets are shown in Figure A.1. The images are then loaded into the open-source ImageJ imaging program to determine the scaling factors for each camera. The targets are held in a 3D-printed target holder that aligns with the holes in the upper insulation to ensure the targets are centered. The tests were performed at normal to the camera and 45° from normal. The exposure and gain for the cameras were adjusted for clarity in the images and the values are summarized in Table A.1. The scaling factor was determined to be 31.70 pixel/mm (805.18 pixel/in.) for the high-speed camera and 63.50 pixel/mm (1,612.90 pixel/in.) for the flame camera. The deployment camera was not calibrated using the targets, but its scaling factor was determined from conversion of the bead diameter when analyzed with the high-speed camera. From this scaling factor, a template was generated to ensure reproducibility in the droplet diameters during deployment. Images with the hook and fiber in its final position for each camera are shown in Figure A.2.

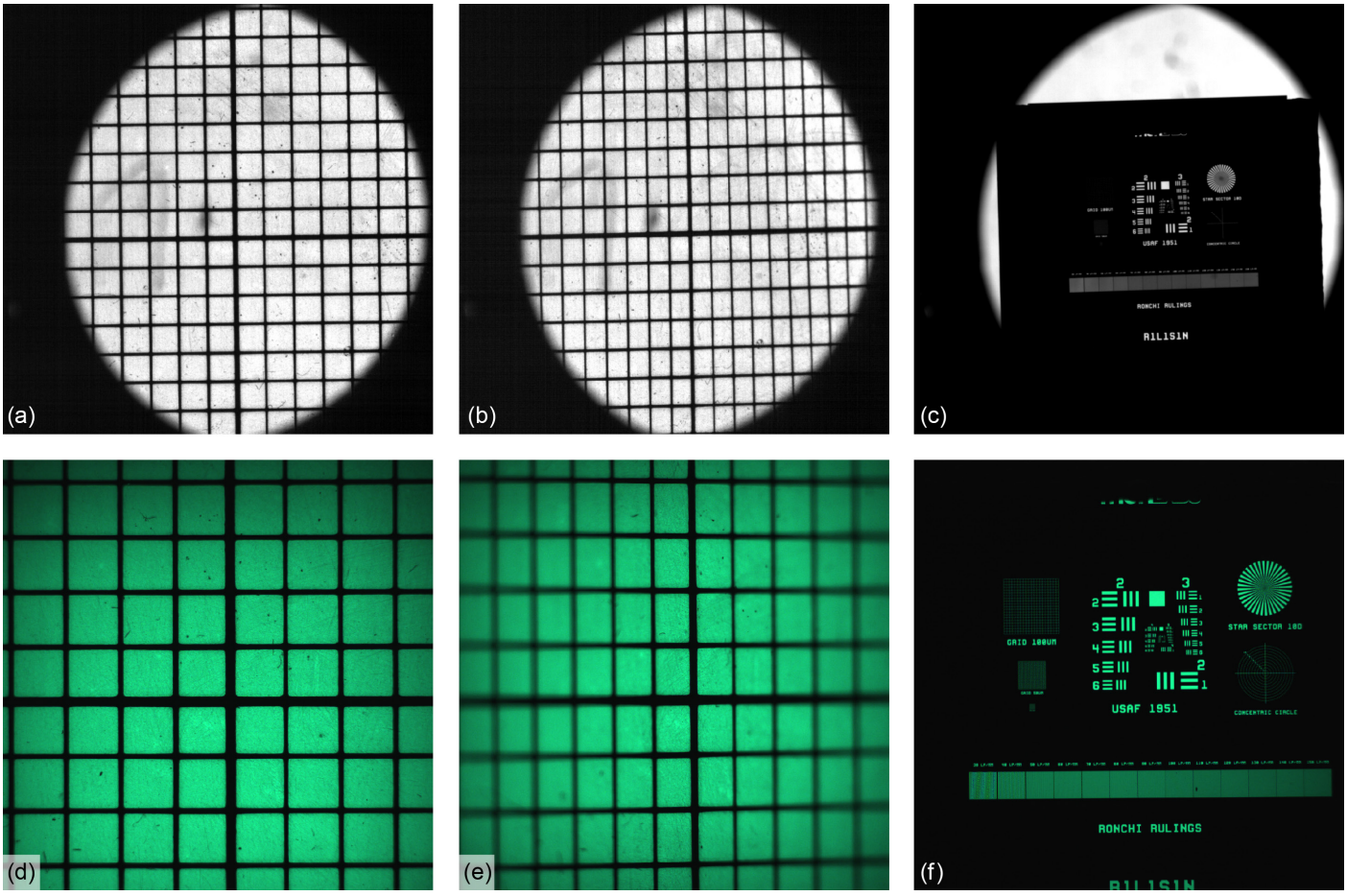

Figure A.1.—Camera targets. (a) 2-mm grid target for high-speed camera aligned normal. (b) 2-mm grid target for high-speed camera aligned 45° from normal. (c) USAF target for high-speed camera aligned normal. (d) 2-mm grid target for flame camera aligned normal. (e) 2-mm grid target for flame camera aligned 45° from normal. (f) USAF target for flame camera aligned normal.

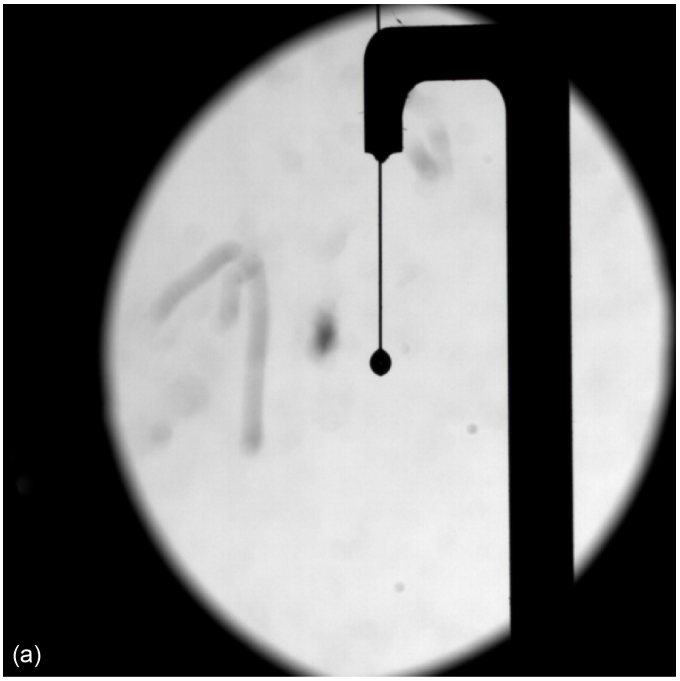

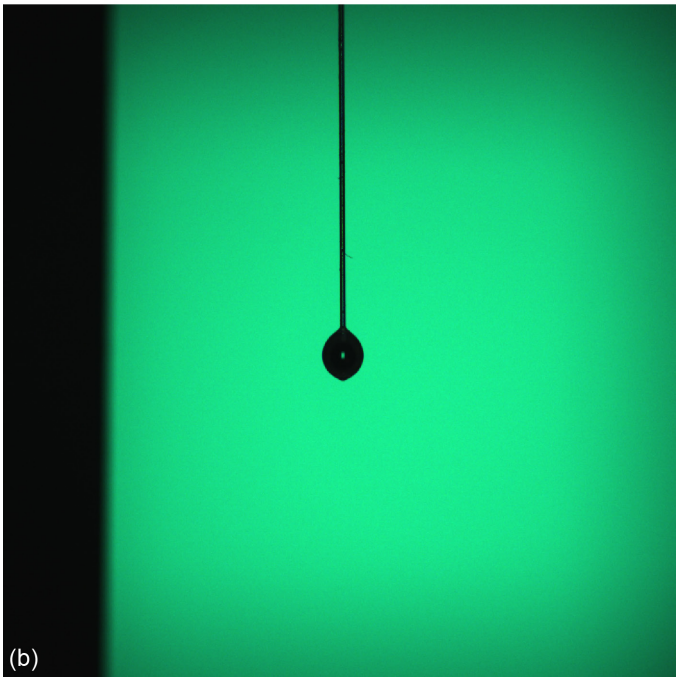

Figure A.2.—Images taken with droplet and hook at final position. (a) High-speed camera image. (b) Flame camera image.

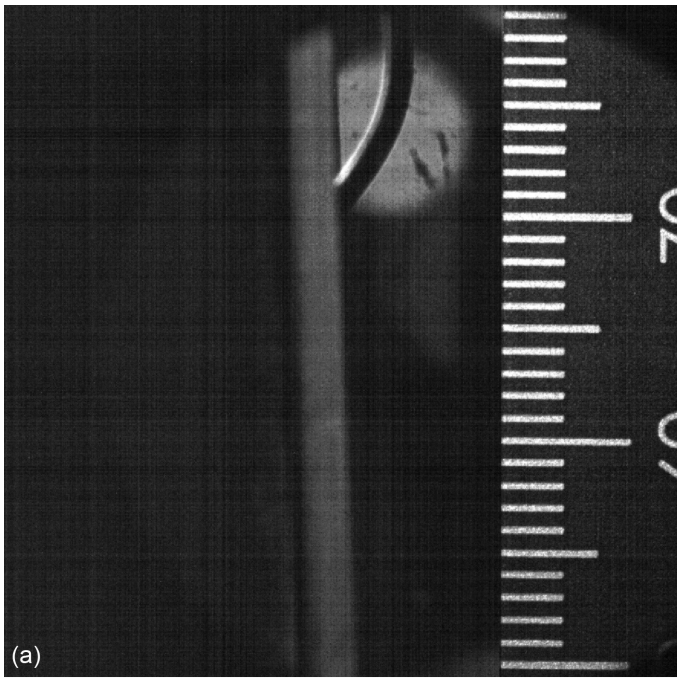

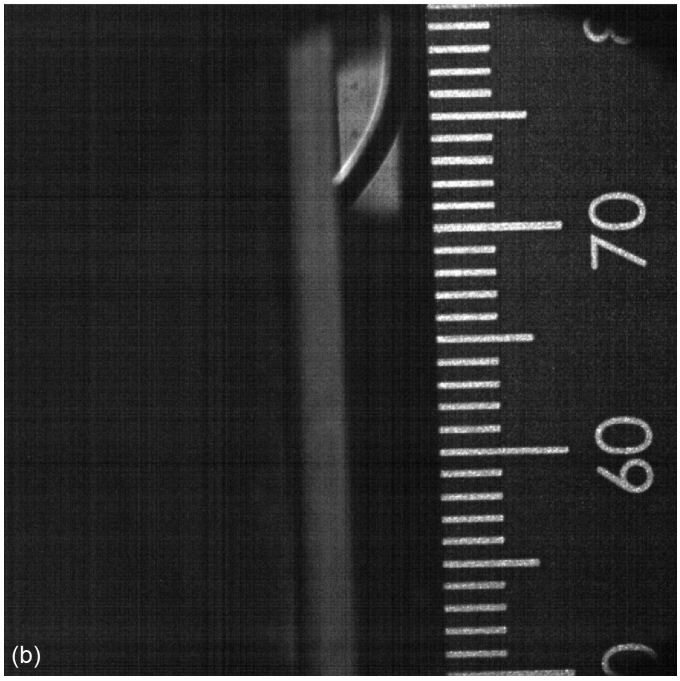

Figure A.3.—Ruler for calculation of distance from entrance of oven to bottom of camera field of view. (a) Aligned ruler. (b) Slanted ruler to verify number values.

In addition to the cameras' scaling factor determinations, the distance from the entrance of the oven to the bottom of each camera's field of view is a required parameter because the camera field of view does not encompass the entire oven. This measurement was determined with a magnetic beam height ruler (Thorlabs) front-illuminated by a very bright green light-emitting diode (LED) and analyzed in the ImageJ program with the known scaling factor for each camera. The value was measured as 49.47 mm (1.948 in.) for the high-speed camera. The values for exposure and gain are shown in Table A.1 and the images are shown in Figure A.3.

TABLE A.1.—CAMERA EXPOSURE AND GAIN FOR TARGET IMAGES

Camera	Target	Gain, dB	Exposure
High-speed	2-mm grid normal	170	999
	2-mm grid 45°	205	999
	USAF target	110	999
	Droplet	94	1,155
	Ruler	417	4,738
Flame	2-mm grid normal	16	488
	2-mm grid 45°	21	488
	USAF target	18	488
	Droplet	16	488

A.2 High-Speed Gain Determination

To enhance the visibility of the cool flame images, the dynamic range of the camera was enhanced. This was done by first adjusting the camera exposure while keeping the gain and black level constant. With the exposure varied from 1 to 1,000 µs with the gain at 50 dB and the black level at 75, still images of the field of view were taken. Histograms of the grayscale values were then calculated, and the range of the camera was determined by the range of the peak values in the histogram. Figure A.4 shows the change in the histogram profile with varying exposures. As can be seen in Figure A.5, there is an optimum exposure value between 400 and 600 µs where the range is maximized. The exposure range is then reduced in steps of 25 µs to obtain a maximum range of 550 to 600 µs; finally, the exposure range is reduced in steps of 5 µs to obtain a maximum range at 570 µs.

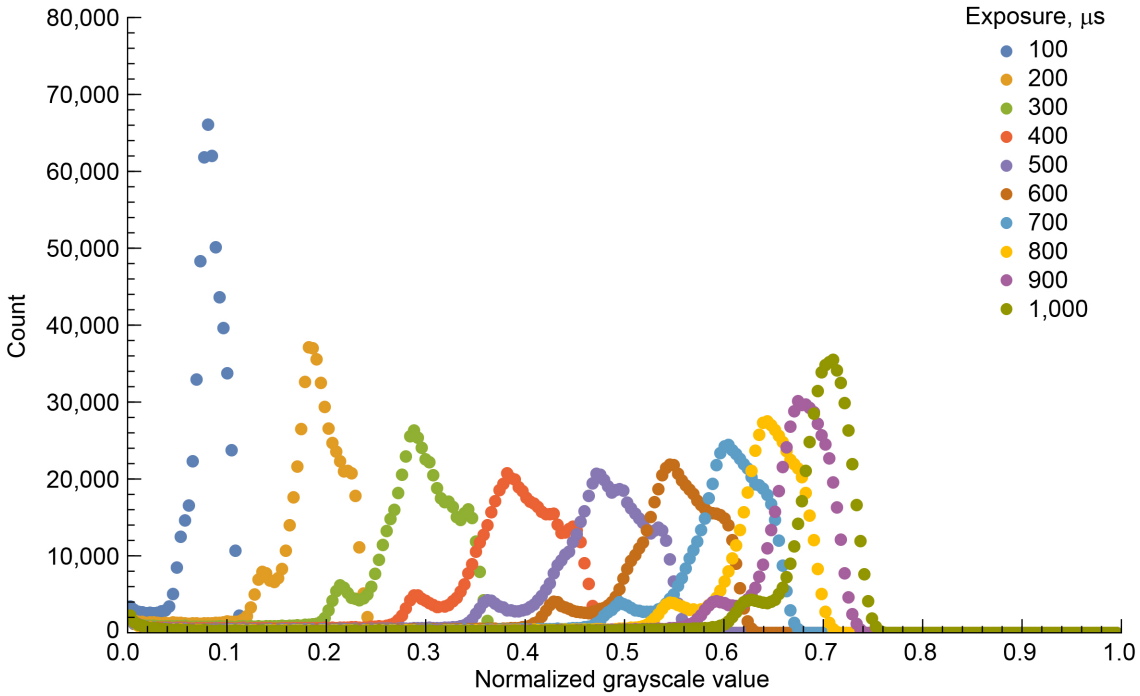

Figure A.4.—Normalized histogram of high-speed image with varying exposures, with 0 corresponding to black grayscale pixel value and 1 corresponding to white pixel.

A similar process is done for the black level, with the exposure fixed at the target exposure of 570 µs. Black level shifts the dynamic range peak to the right towards higher grayscale values, as seen in Figure A.6. Given that the black level has no impact on the range of the peak, the lowest value of 0 is chosen for the black level to allow for a higher inclusion of gain without oversaturating the camera. It should be noted that a second peak occurs at the low grayscale values, which corresponds to the black values seen on the edges of the images around the window. The peak occurred previously, but it was contained to a single pixel value with a count that was beyond the range of the previously plotted results. Because the increasing black level broadens this lower peak (as these values are black), the values are now visible on the plot.

Finally, the values for the gain are adjusted. As shown in the histograms in Figure A.7, increasing the camera gain increases the peak range and shifts the peak to the right towards brighter grayscale values. The camera saturates at gain values greater than 100 dB. Although increasing camera gain increases noise in the signal, Figure A.8 clearly shows that increasing gain largely increases the dynamic range of the camera. To reduce the signal noise to some degree, a gain value of 80 dB is chosen to optimize peak range without introducing too much noise into the signal.

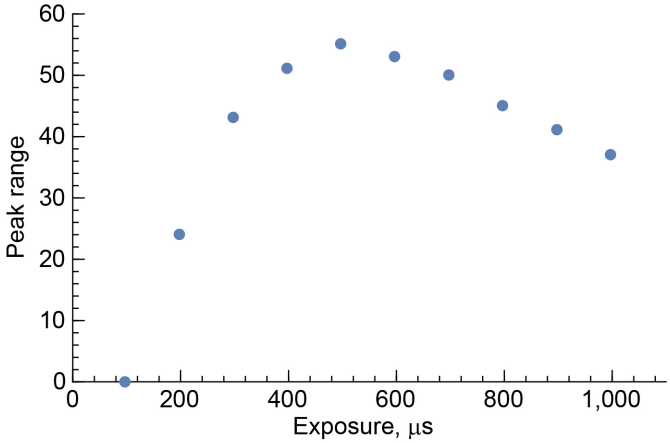

Figure A.5.—Range in peak of normalized histogram of high-speed image with varying exposures.

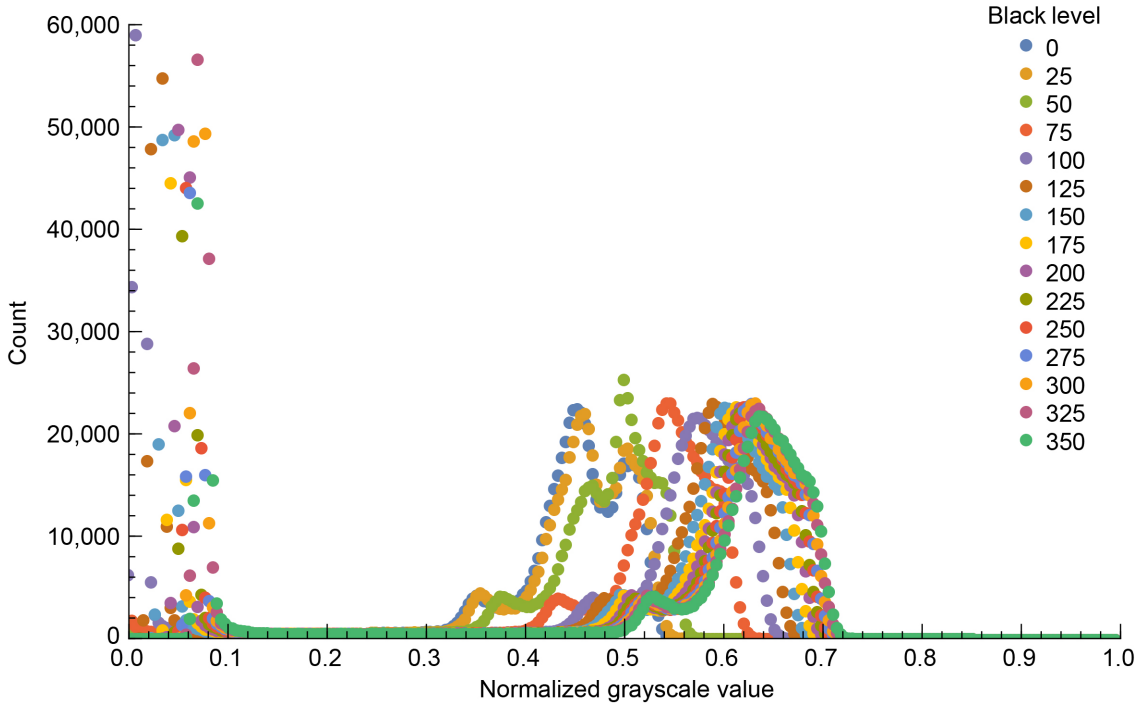

Figure A.6.—Normalized histogram of high-speed image with varying black level with 0 corresponding to black grayscale pixel value and 1 corresponding to white pixel.

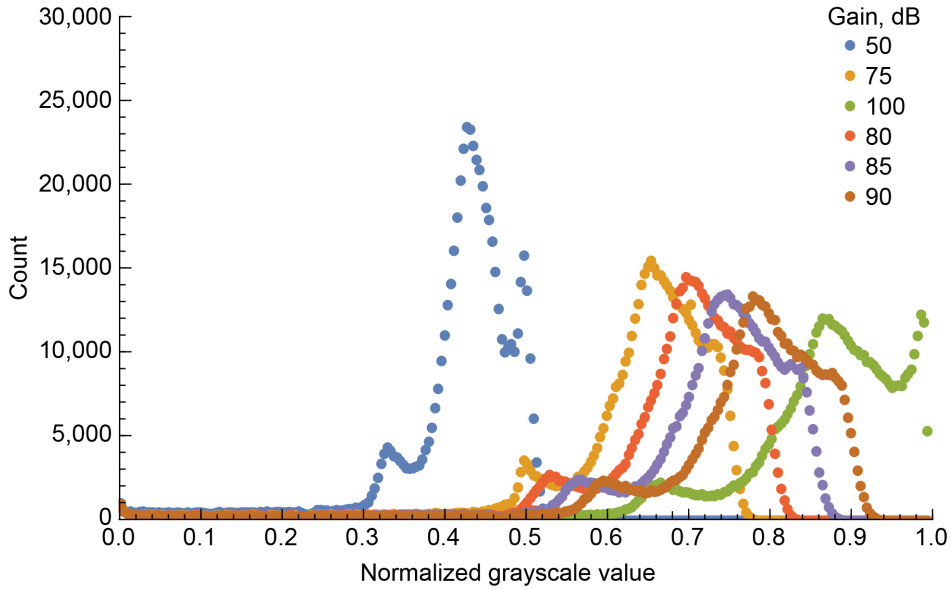

Figure A.7.—Normalized histogram of high-speed image with varying gain with 0 corresponding to black grayscale pixel value and 1 corresponding to white pixel.

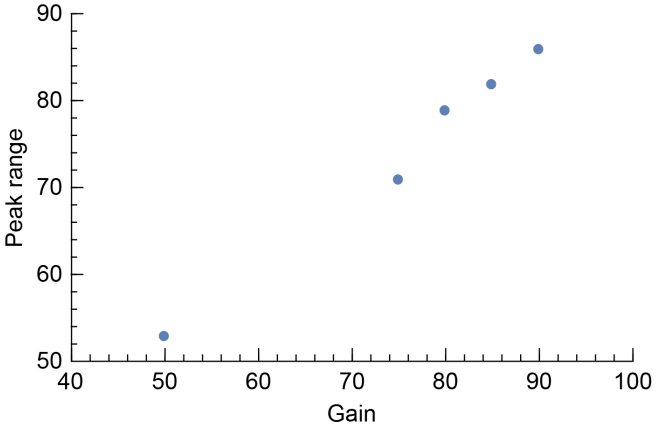

Figure A.8.—Range in peak of normalized histogram of high-speed image with varying gain.

A.3 Stepper Motor Characterization

To verify reproducibility in the insertion times of the insertion profile and velocities, the translation of the stepper cart into the oven is characterized. In the analysis procedure, linear extrapolation is used to determine the time of entry of the droplet into the chamber because this occurs outside of the field of view of the high-speed camera. To verify that this translation is linear throughout its travel distance, the full translation is captured using the video camera in a smartphone (iPhone 10) at 240 fps. The smartphone is mounted on a tripod and positioned at normal to the flame camera (45° from normal with respect to the hook) and at 45° from normal from the flame camera (normal with respect to the hook). An 8-mm (0.31-in.) scaling sticker (PGC Scientifics 50–1664–14) is placed on the hook to allow for scaling and for an easily identifiable point to track during the translation. A yellow sticker is placed at 8.2 mm (0.323 in.) below the droplet; a second black sticker is placed at 20.7 mm (0.815 in.) below the droplet. Cropped images for the start, middle, and end of the translation are shown in Figure A.9.

The scaling factor for the images is deduced from the 8-mm (0.31-in.) sticker. For the normal tests, the scaling factor is 3.75 pixel/mm (95.25 pixel/in.); for the 45° from normal tests, the scaling factor is 4 pixel/mm (101.6 pixel/in.). The tests are then analyzed by tracking the yellow sticker, which is accomplished by subtracting the blue image channel from the average of the red and green image channels. This subtraction yields an image that only contains the yellow dot. This dot is then tracked throughout the translation by thresholding the image, then analyzing the particle. The location of the centroid of the particle is tracked and converted to the droplet position using the known vertical distance between the sticker center and the droplet location. Figure A.10 shows a representative curve. The translation occurs in two parts, the first being the approach where the cart translates vertically until it hits the limit switch, just before the entrance into the oven. After a 100-ms delay, the second portion begins, which is the translation of the cart into the oven. The linear region of the curve is then fit using linear regression and the value for the approach speed and translation speed is taken. This process is repeated for four normal tests and three 45° from normal tests; the results of each test are shown in Table A.2. The speed is averaged between the tests for an approach speed of 161.40 mm/s (6.354 in./s) and a translation speed of 162.36 mm/s (6.392 in./s). This value matches well with the anticipated slopes of the high-speed analysis. Due to the linearity of the translation, as seen in Figure A.10, the extrapolation for the determination of the time of droplet entry into the chamber is justified.

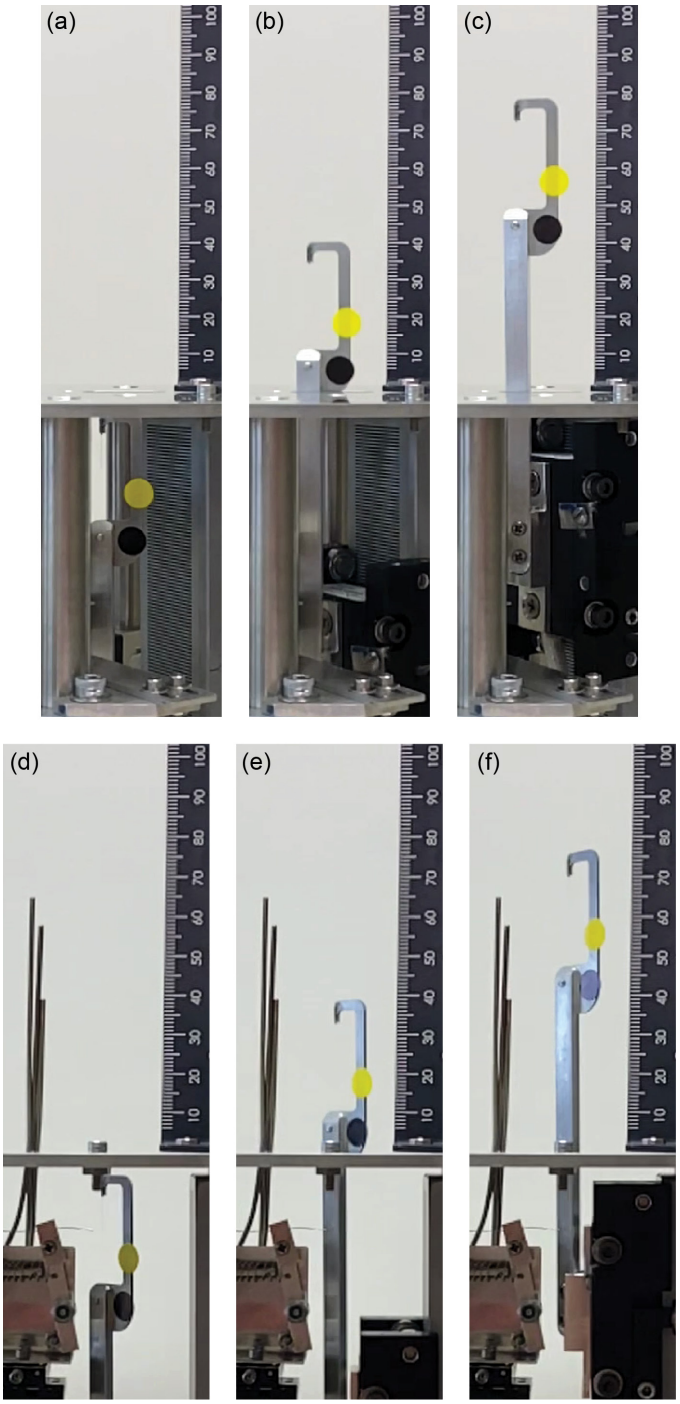

Figure A.9.—Translation of droplet. (a) Hook at start of translation for 45° from flame camera normal (normal with respect to hook). (b) Hook during translation for 45° from flame camera normal (normal with respect to hook). (c) Hook at end of translation for 45° from flame camera normal (normal with respect to hook). (d) Hook at start of translation for flame camera normal (45° from normal with respect to hook). (e) Hook during translation for flame camera normal (45° from normal with respect to hook). (f) Hook at end of translation for flame camera normal (45° from normal with respect to hook).

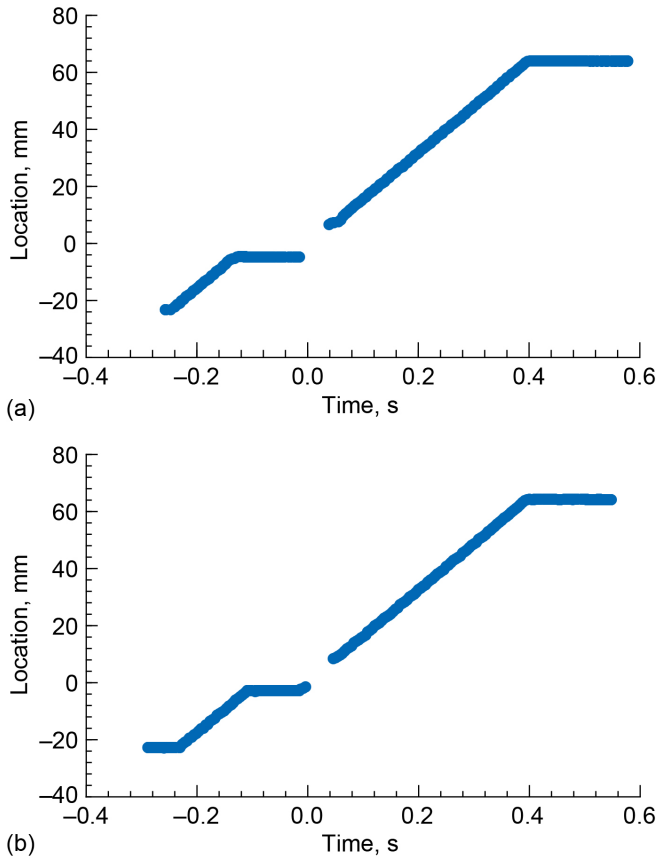

Figure A.10.—Vertical displacement versus time where 0 s corresponds to entrance of droplet into oven and 0 mm corresponds to bottom of the oven. (a) 45° from flame camera normal (normal with respect to hook) case. (b) Flame camera normal (45° from normal with respect to hook) case.

TABLE A.2.—APPROACH SPEED AND TRANSLATION SPEED FOR EACH TEST

Test	Orientation (WRT flame camera)	Approach speed, mm/s	Translation speed, mm/s
001	Normal	163.51	162.31
002		159.66	162.15
003		161.91	162.10
004		161.26	162.04
005	45° from normal	No test	No test
006		161.04	162.69
007		160.87	162.58
008		161.58	162.62
Mean		161.40	162.36

A.4 Temperature Characterization

An ideal case of droplet autoignition would require a perfectly insulated oven at a uniform temperature. Given that the experimental conditions are not ideal, characterization of the temperature gradients within the oven becomes critical. The oven is characterized using multiple Type K thermocouples positioned throughout the heated portion of the chamber. Various tests were run at multiple heater setpoints and pressures to determine the temperature distribution both radially and vertically. Because the heaters pulse on and off and there is a heat-up and cool-down component to the testing sequence, the temperature distribution will have a temporal component as well. To resolve the temporal component of the temperature distribution, four thermocouples were positioned on the hook at various vertical locations, and the cart was held at its final position, as shown in the high-speed image in Figure A.11 with positions outlined in Table A.3. Using these thermocouples in concurrence with the permanent thermocouples in the rake (TC–1 to TC–3) allows approximating the vertical and radial temperature profile in the oven. As seen in Figure A.12, the temperatures converge radially after the heaters turn off and the vertical temperature distribution decreases, which justifies the decision to let the heaters decay before conducting the test. Additionally, as the heaters pulse to maintain temperature, allowing the temperature to decay before the tests eliminates flows caused by oscillations from the heaters. Note that the rate of decay of the oven temperature is faster for higher temperature setpoints.

The temperature distribution at the point of test initiation is of particular interest. When the setpoint reaches the desired temperature after a 100-K decay with the heaters turned off, the test sequence begins. Using the thermocouples in the permanent rake, and by positioning the thermocouples on the hook at the final position and keeping them stationary, the temperature gradient during the test sequence can be characterized. As can be seen in Figure A.13, there is both a radial and vertical dependence of temperature with location. In the vertical direction near the droplet (r = 0 mm), the gradient is about 2.5 K/mm (114 °F/in.); near the wall (r = 24.8 mm or 0.976 in.), the gradient is about 1 K/mm (45.7 °F/in.). In the radial direction, at the droplet height, the gradient is about 0.5 K/mm (22.9 °F/in.). These gradients are relatively insensitive to the setpoint temperatures.

The full temperature profile in the oven is determined by translating the stepper motor upwards at the start of the test. The stepper motor is translated in 2-mm (0.079-in.) increments with a time step of 1 s at each height. The full translation takes approximately 40 s. The temperatures are then determined by using the temperature of the open junction thermocouple (TC–11) at the top of the hook to allow for the largest range within the oven and the fastest response time. The full characterization is shown in Figure A.14; note that the steepest gradient occurs at the entrance to the oven and begins to flatten out near the droplet. Increased pressures have slightly steeper temperature gradients at the entrance of the oven but, when compared to lower pressures, tend to flatten out more at lower heights. Because the temperature decay is highly transient, some differences will occur throughout the 40 s of translation of the stepper motor. The solid lines in the figure denote the temperatures from the stationary hook thermocouples (as shown in Figure A.13) and are included to indicate the more appropriate temperature values near the droplet at the start of the test. As can be seen, the differences between the solid lines and the dashed lines are greater at the higher setpoint temperatures because the temperature decay is happening at a faster rate at higher setpoint temperatures.

TABLE A.3.—LOCATIONS OF THERMOCOUPLES USED FOR CHARACTERIZATION

Thermocouple	z, mm	r, mm	Type
TC–8	54	0	Ungrounded
TC–9	58	0	
TC–10	65	0	
TC–11	70.5	0	Exposed

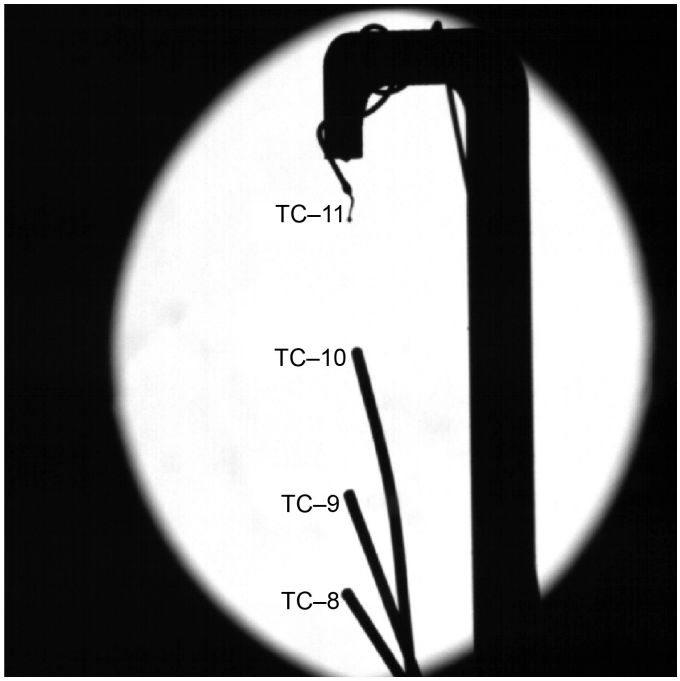

Figure A.11.—High-speed camera image showing locations of thermocouples attached to hook.

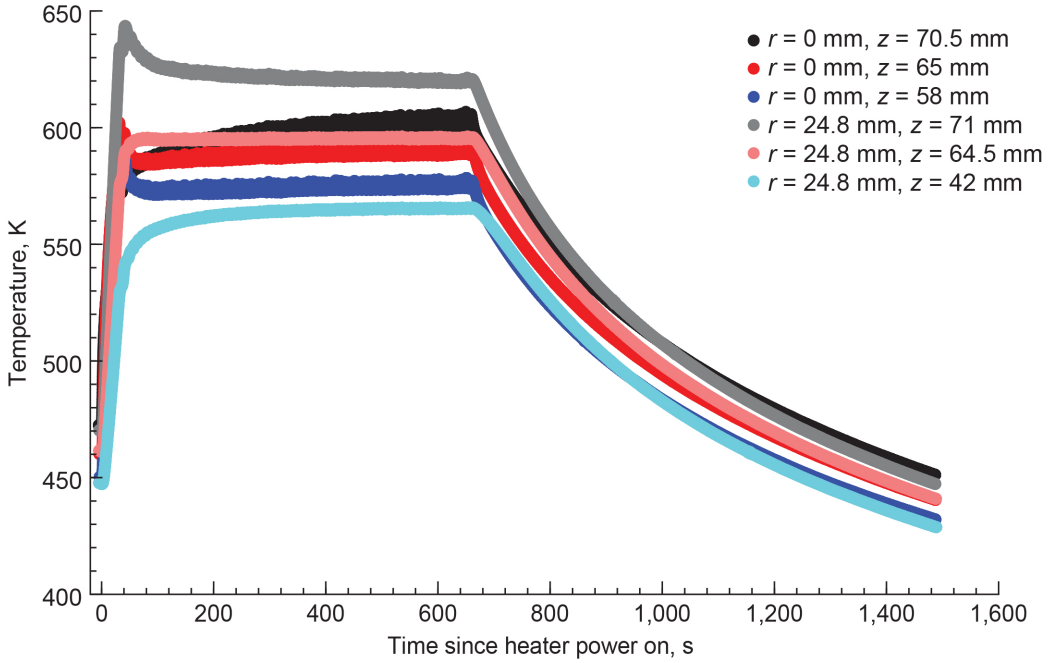

Figure A.12.—Temperature profile with time at various locations throughout oven in vicinity of droplet height.

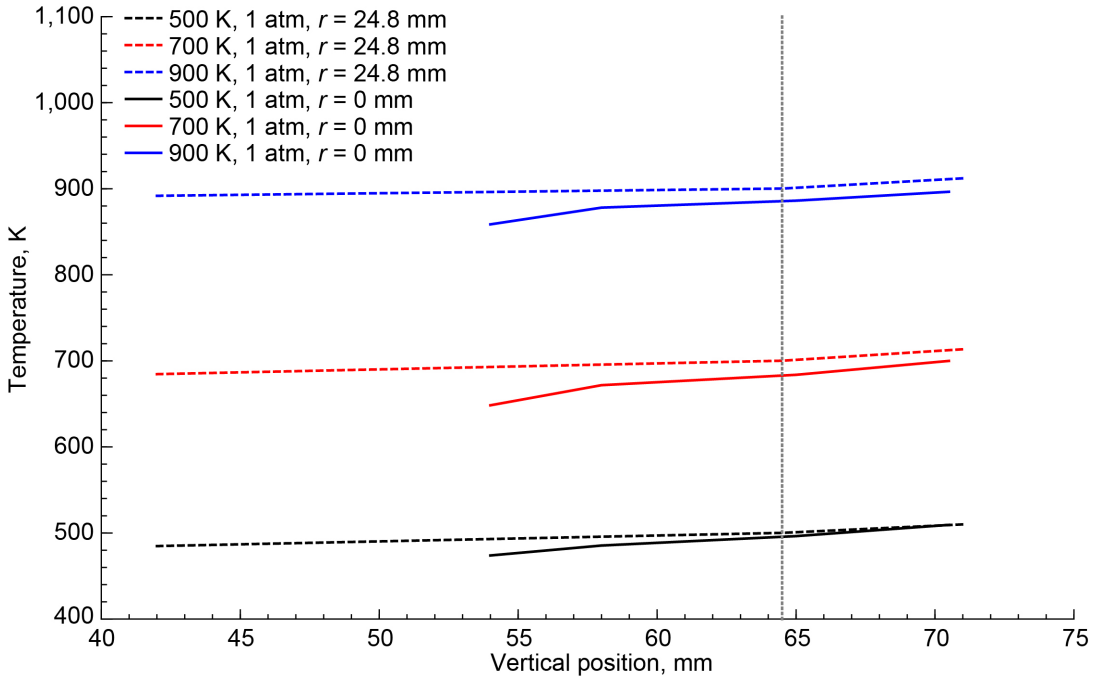

Figure A.13.—Temperature profile at time of test sequence at various locations throughout oven in vicinity of droplet height. Dashed line indicates droplet final position.

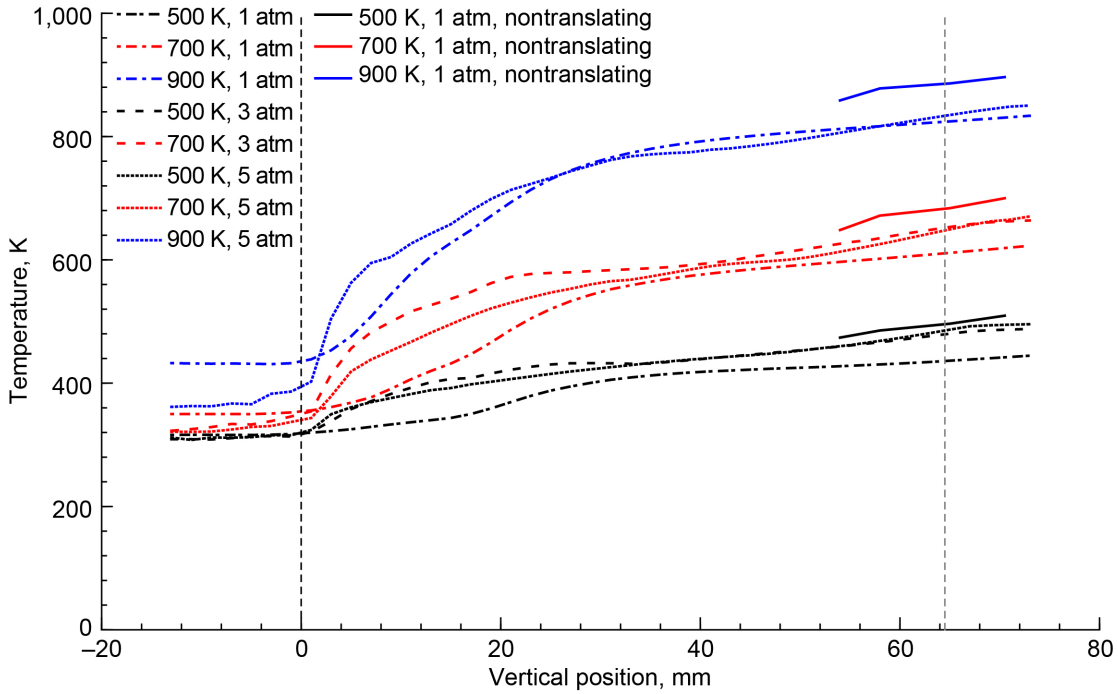

Figure A.14.—Temperature profile throughout oven. Dashed lines indicate entrance of oven (0 mm) and droplet final position (64.5 mm or 2.54 in.).

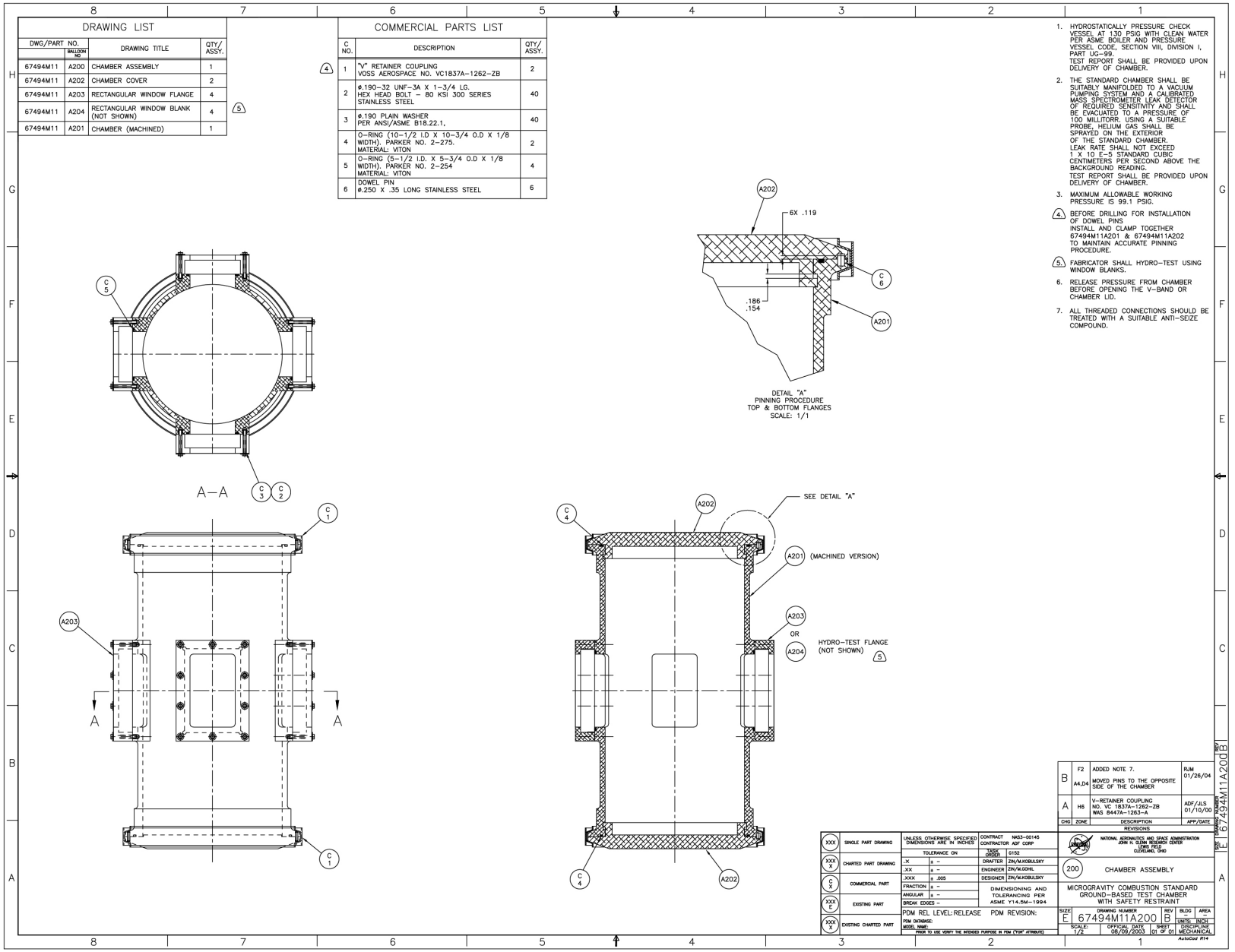

Figure B.1.—Chamber assembly.

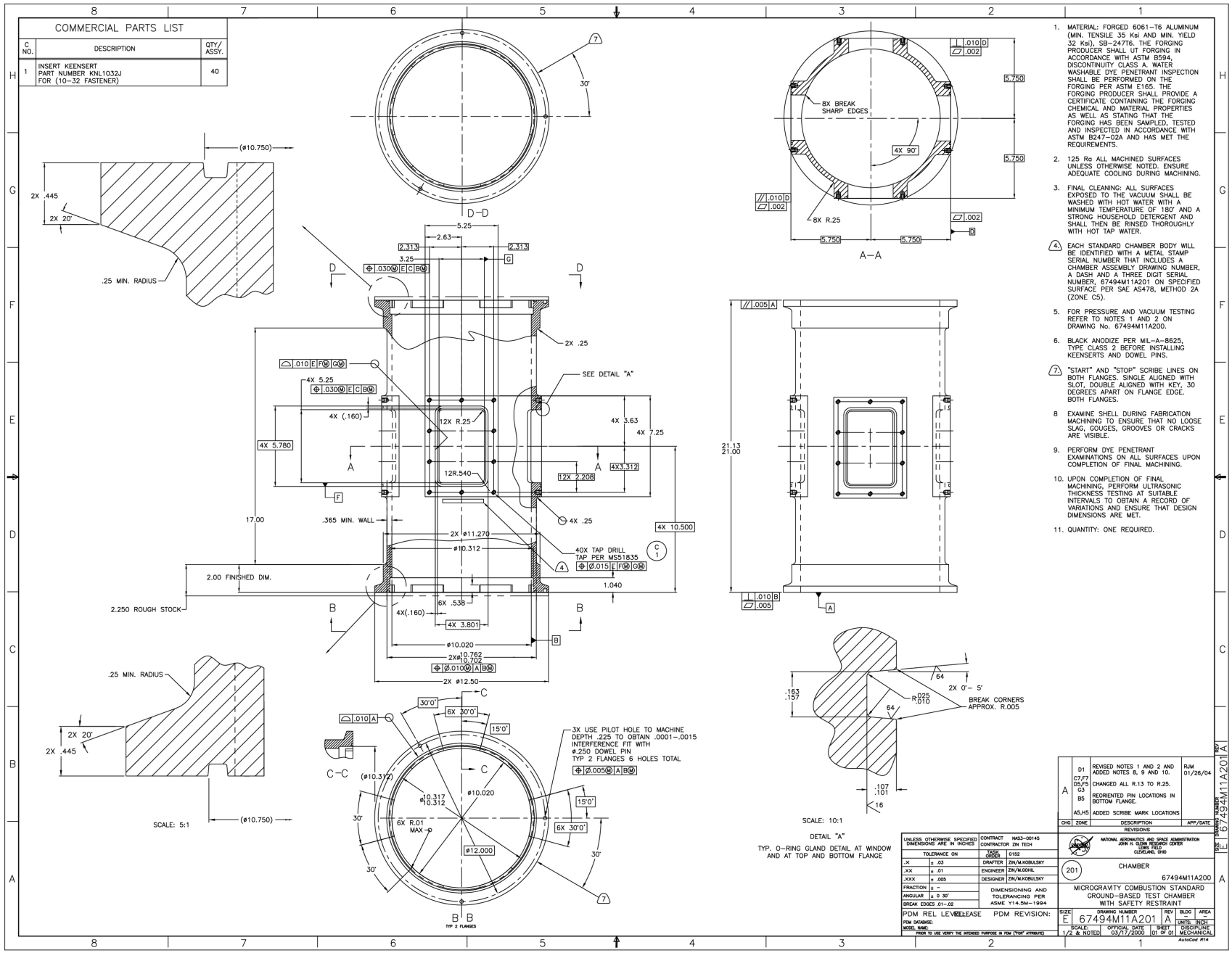

Figure B.2.—Chamber.

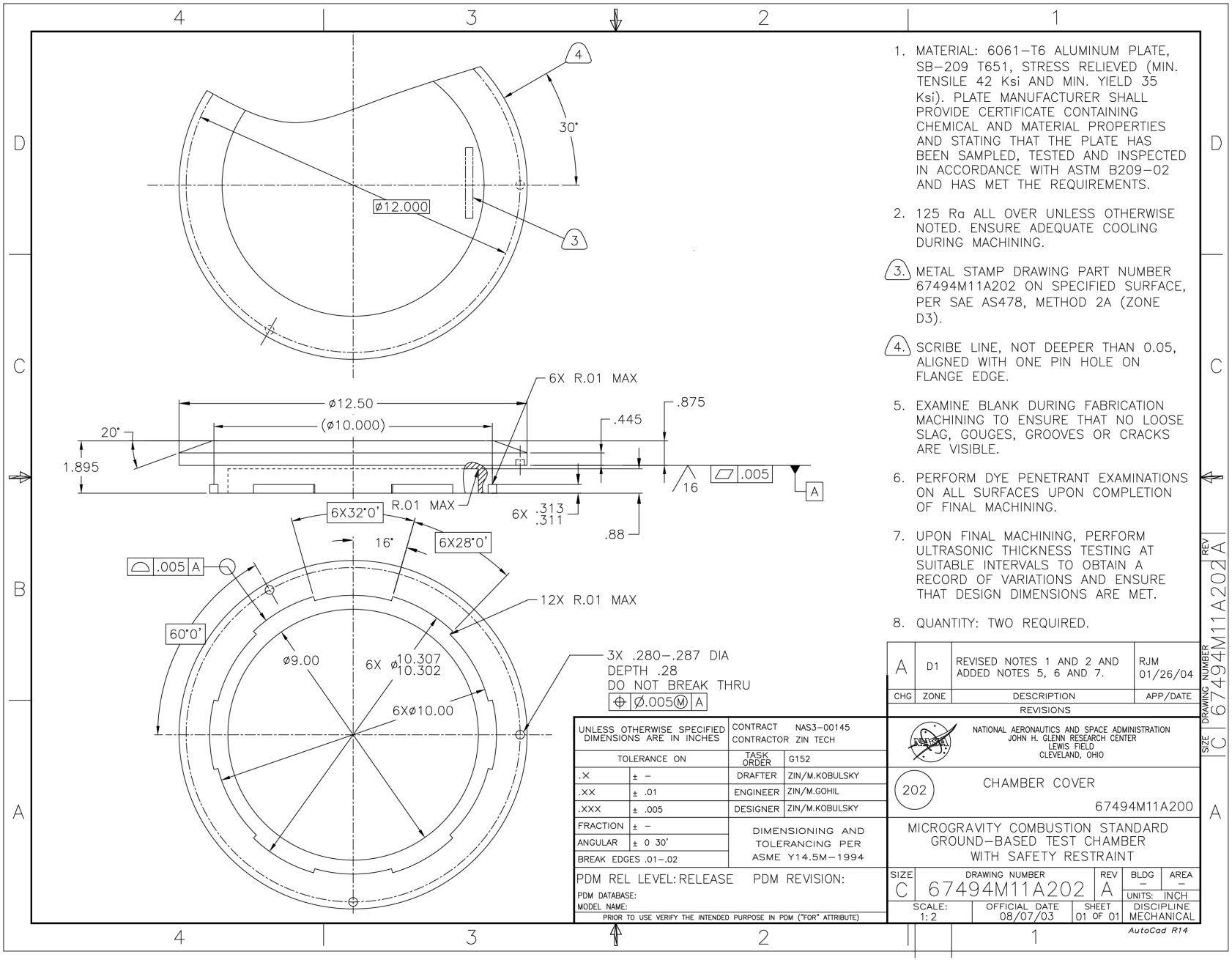

Figure B.3.—Chamber cover.

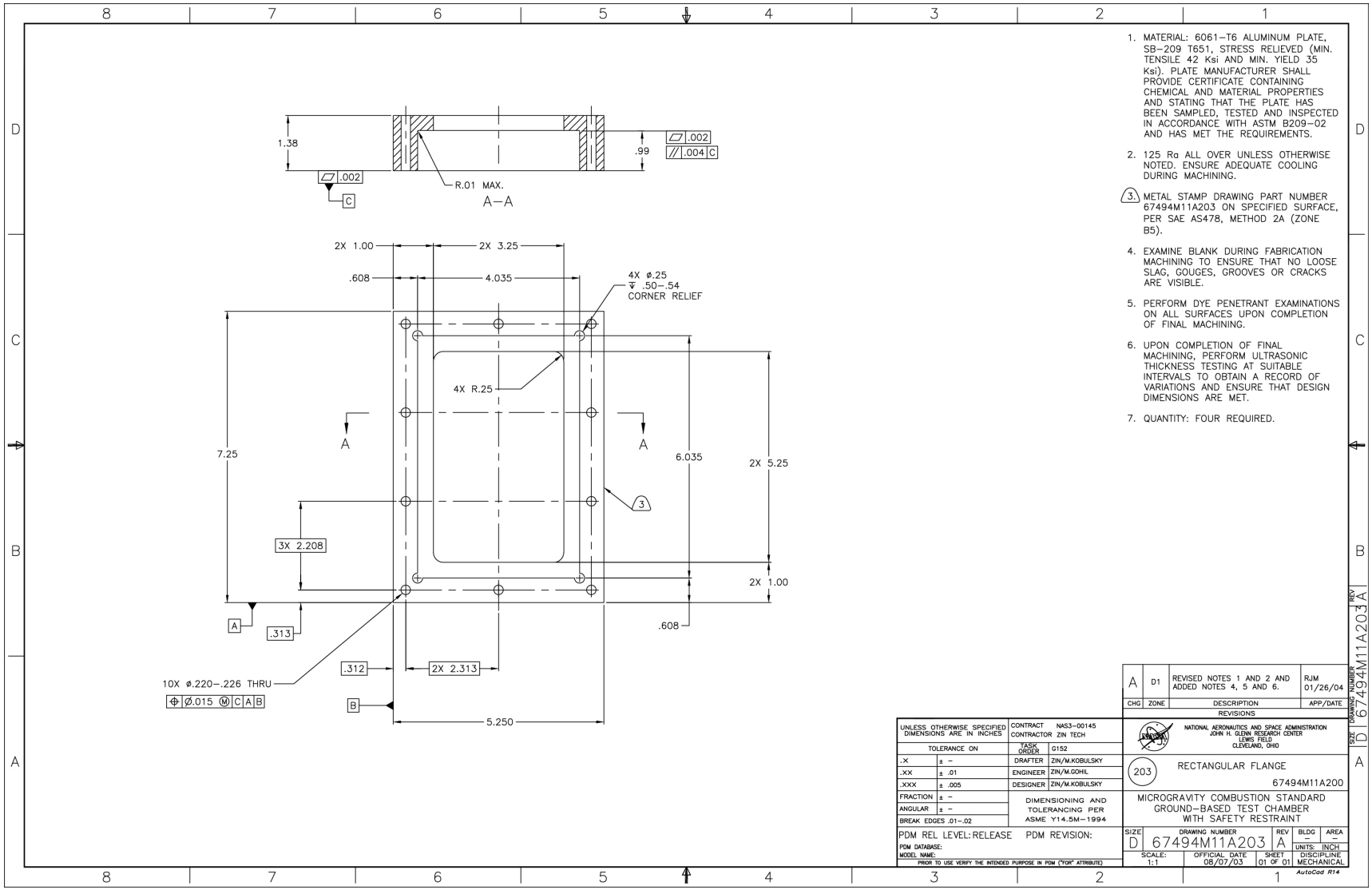

Figure B.4.—Window flange.

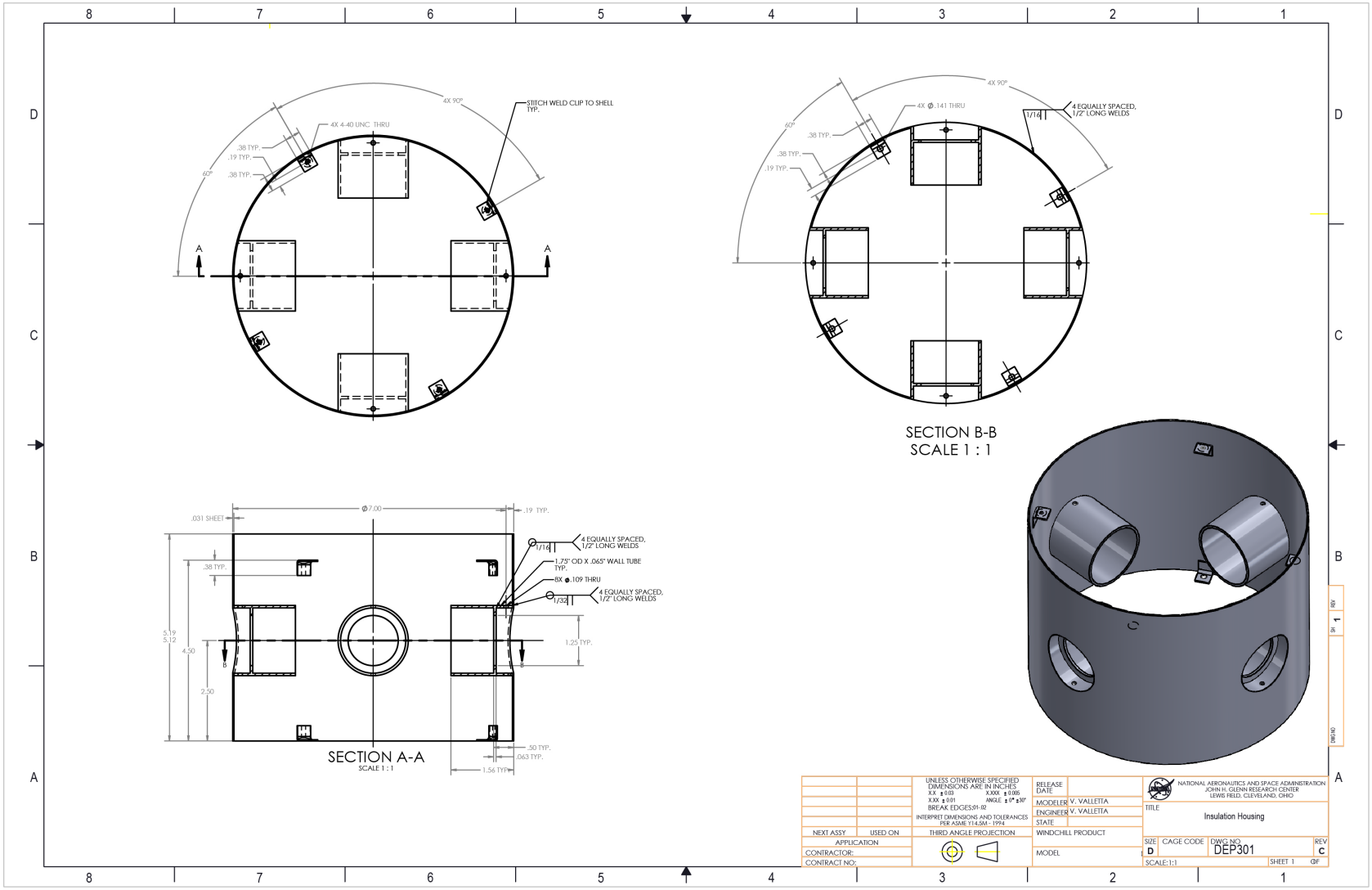

Figure B.5.—Insulation housing.

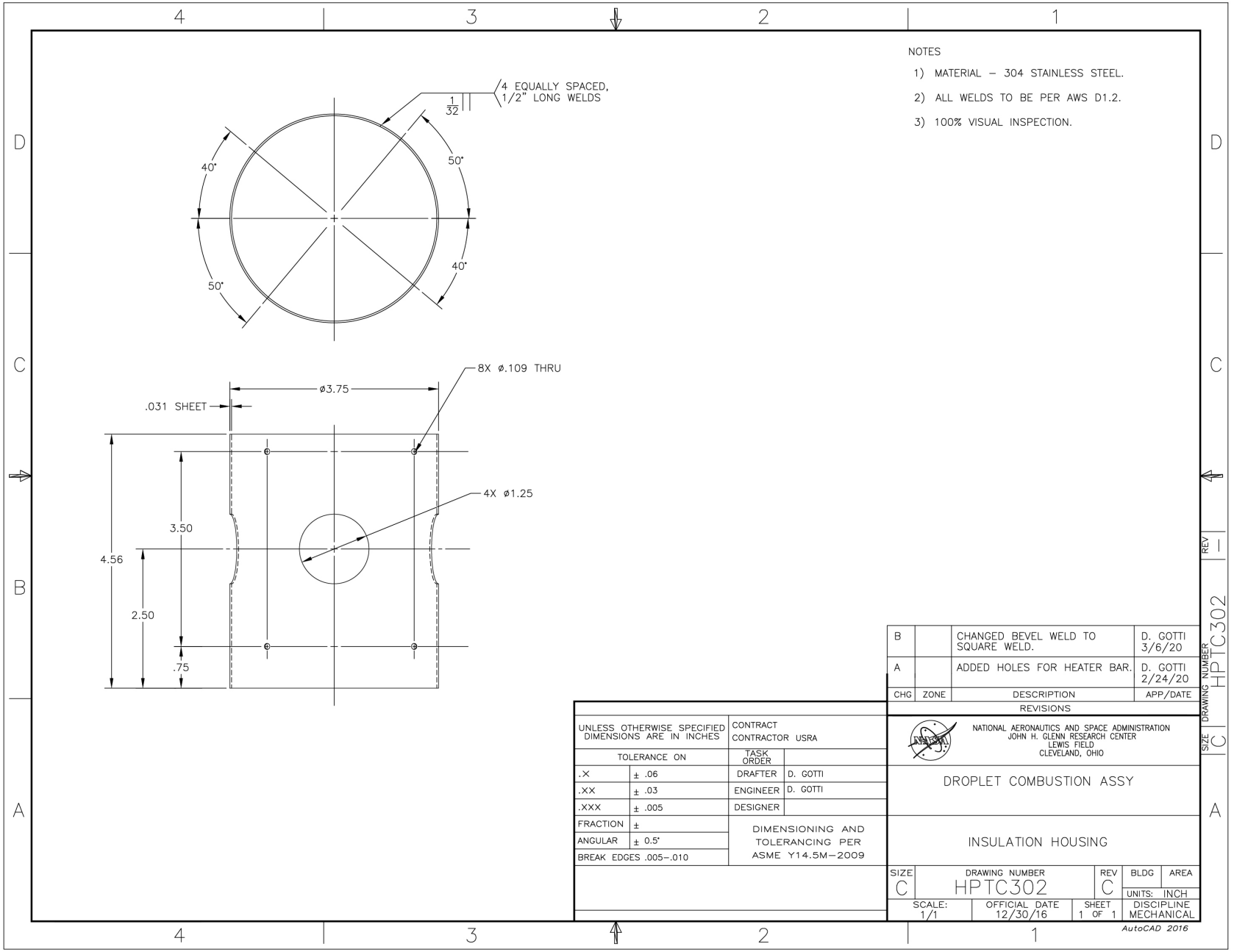

Figure B.6.—Heater housing.

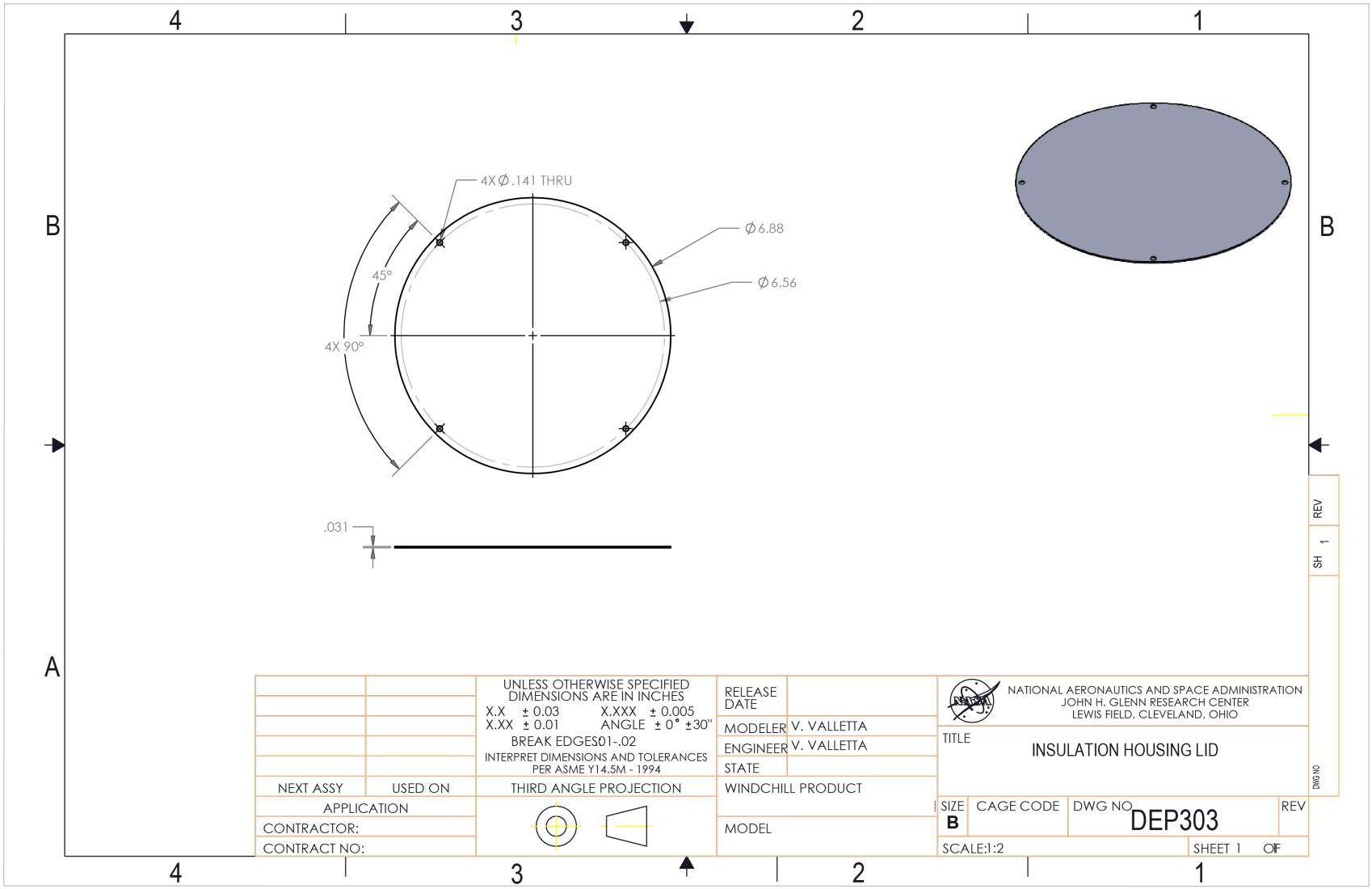

Figure B.7.—Insulation housing lid.

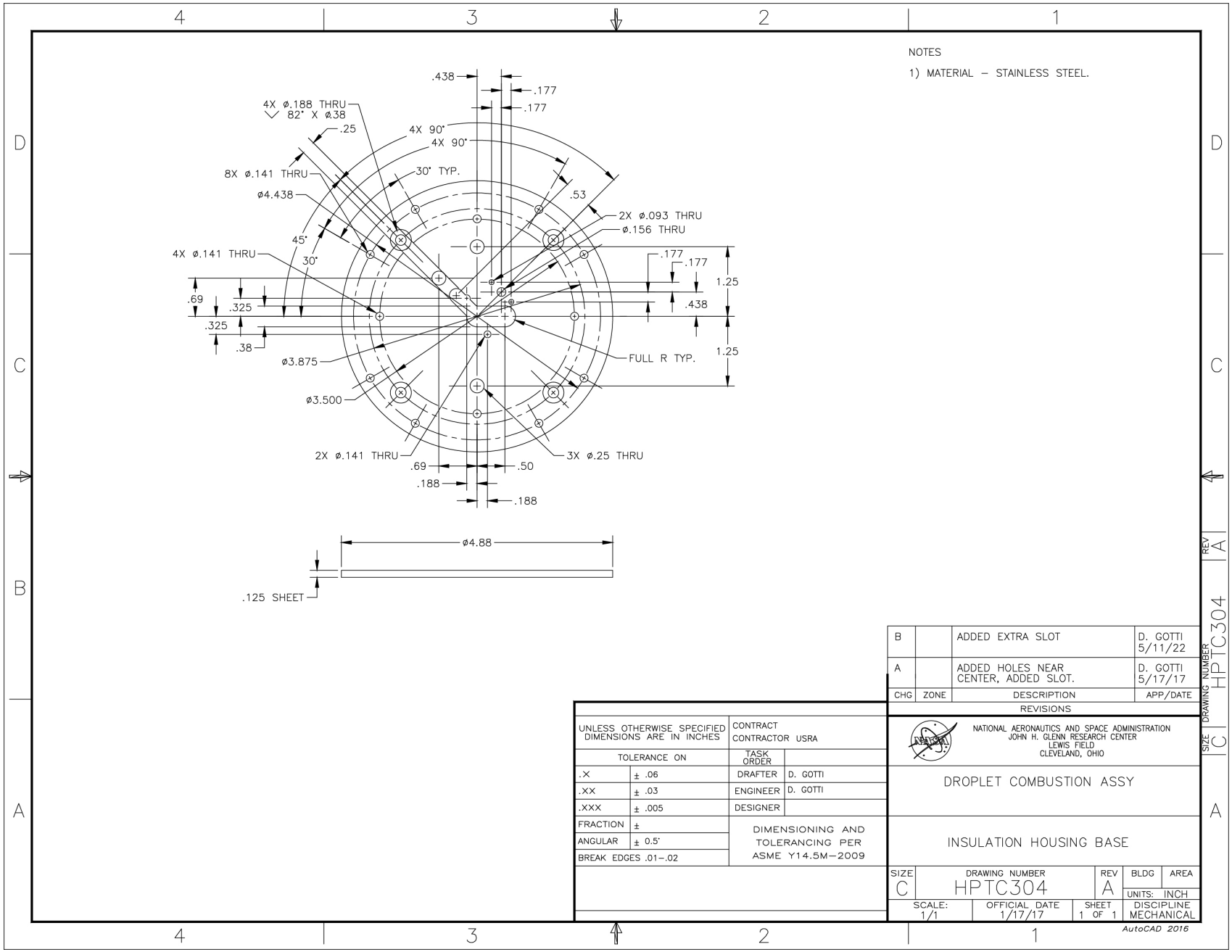

Figure B.8.—Insulation housing base.

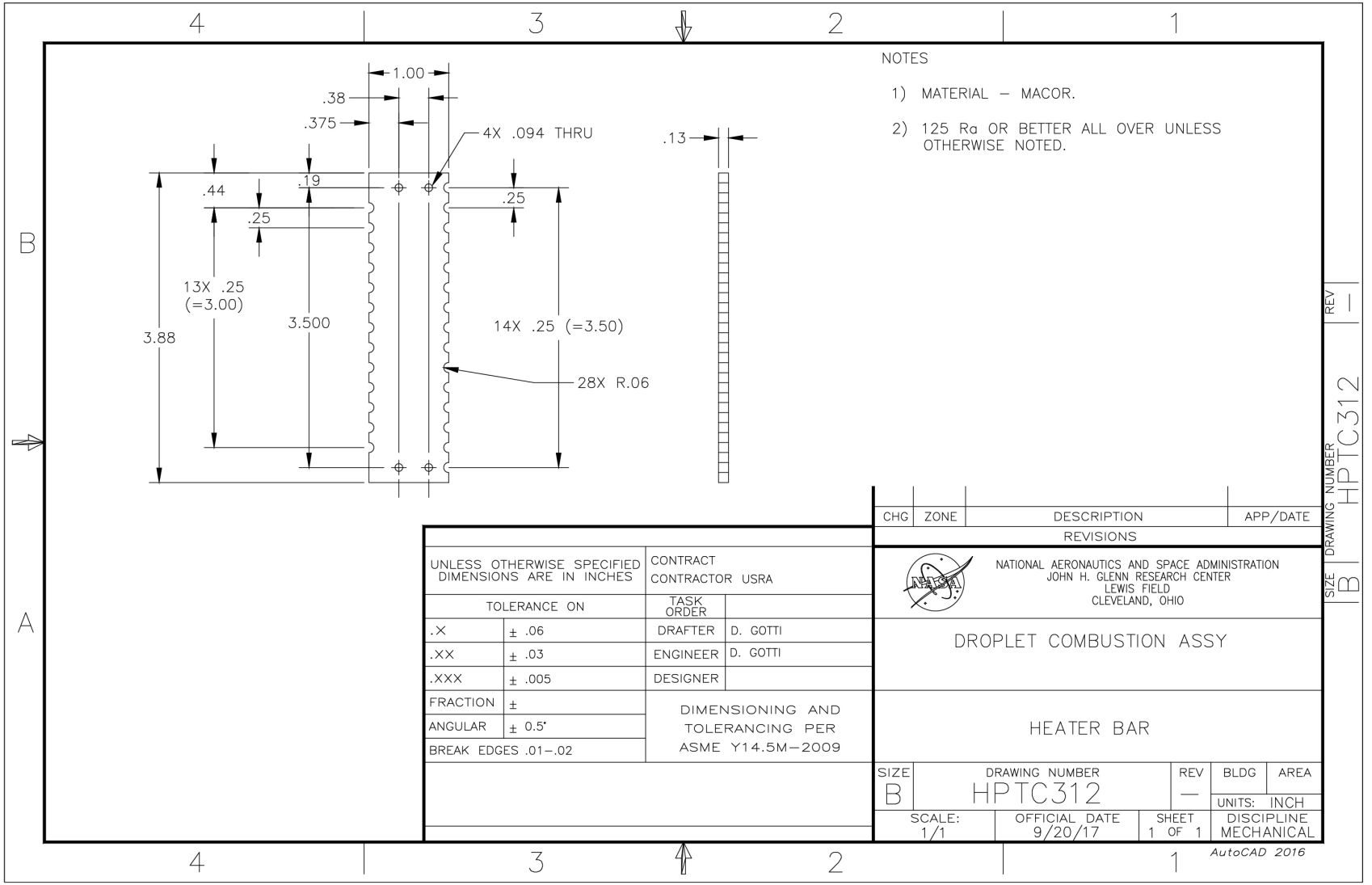

Figure B.9.—Heater bar.

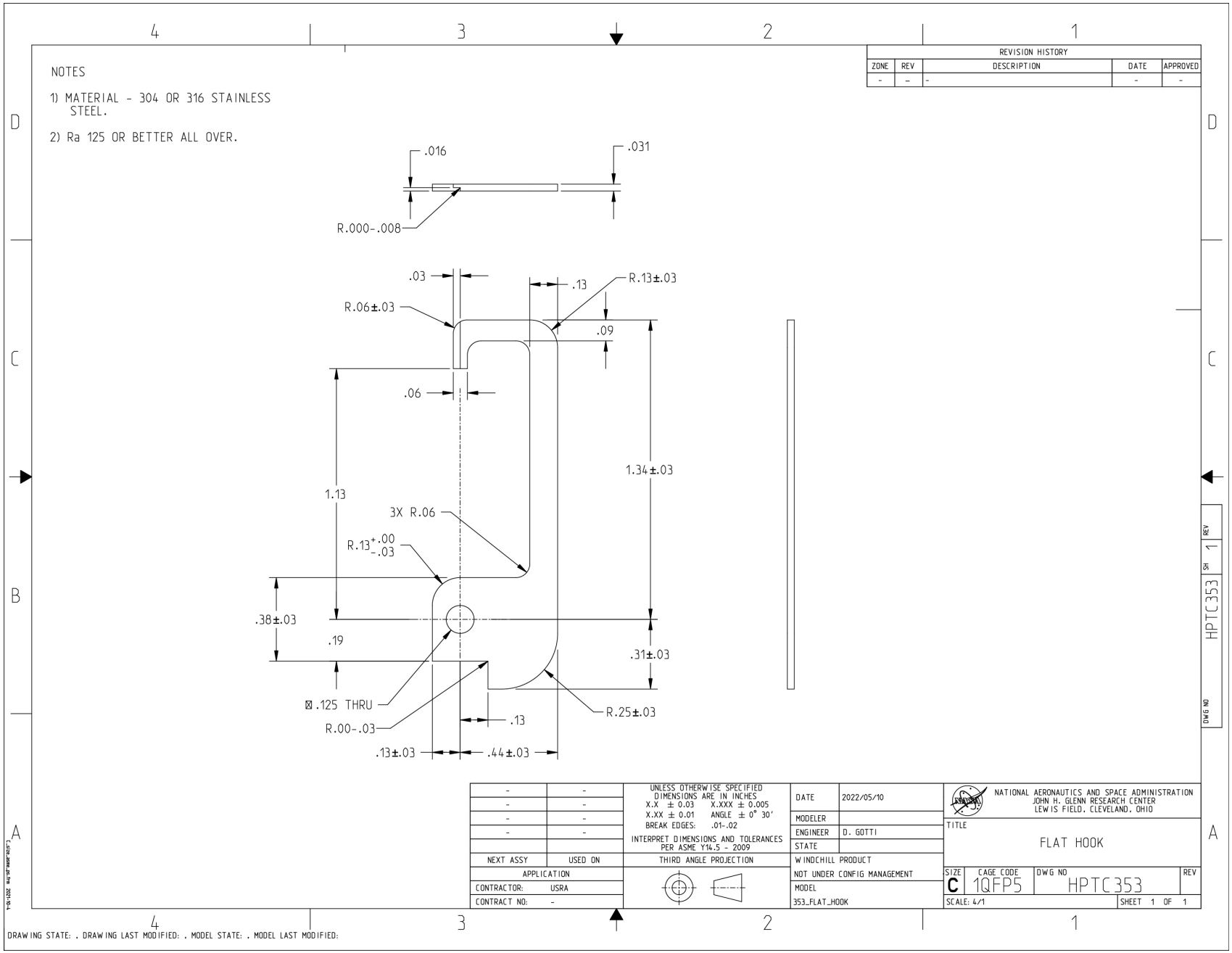

Figure B.10.—Fiber hook.

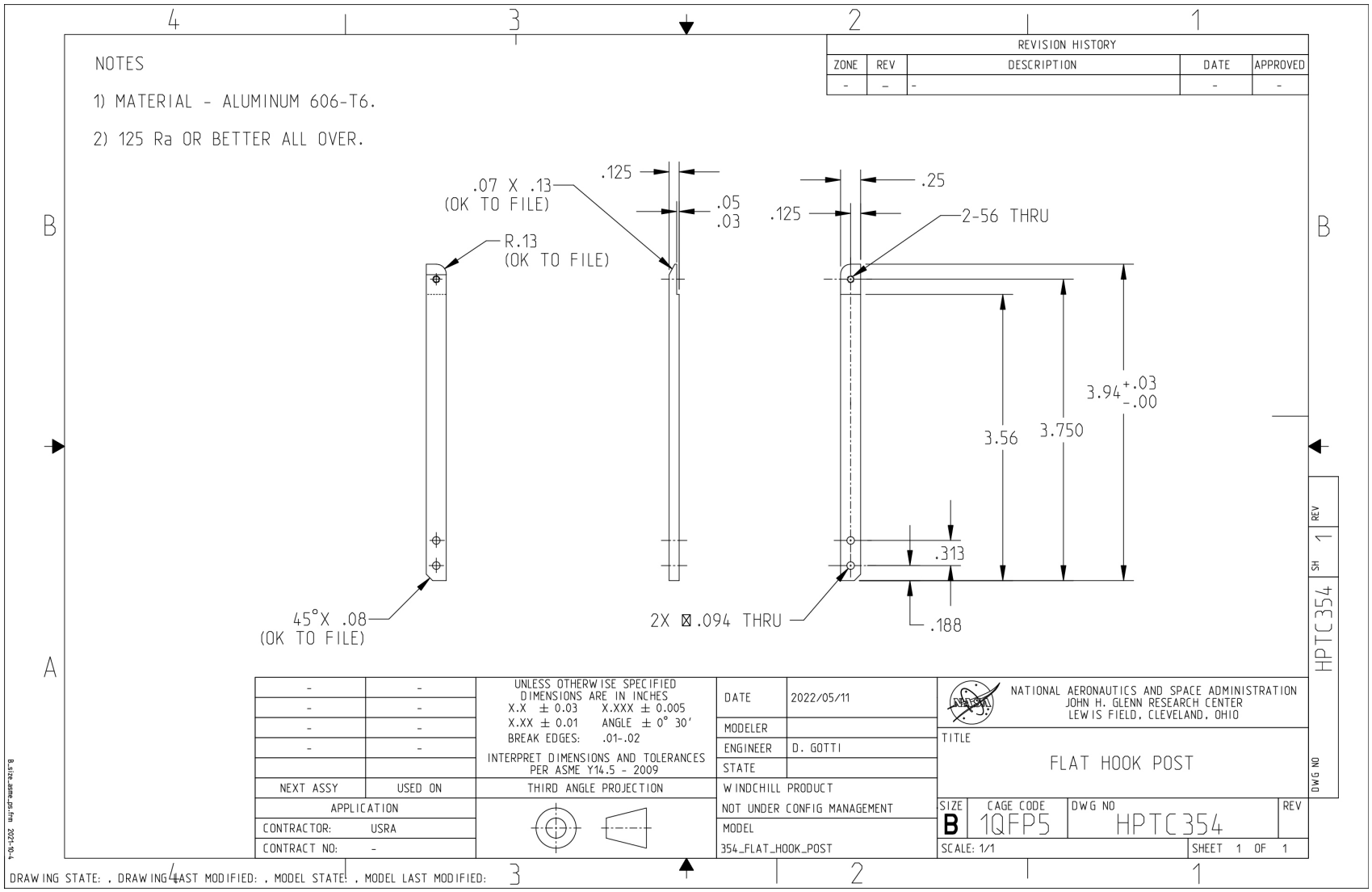

Figure B.11.—Fiber hook post.

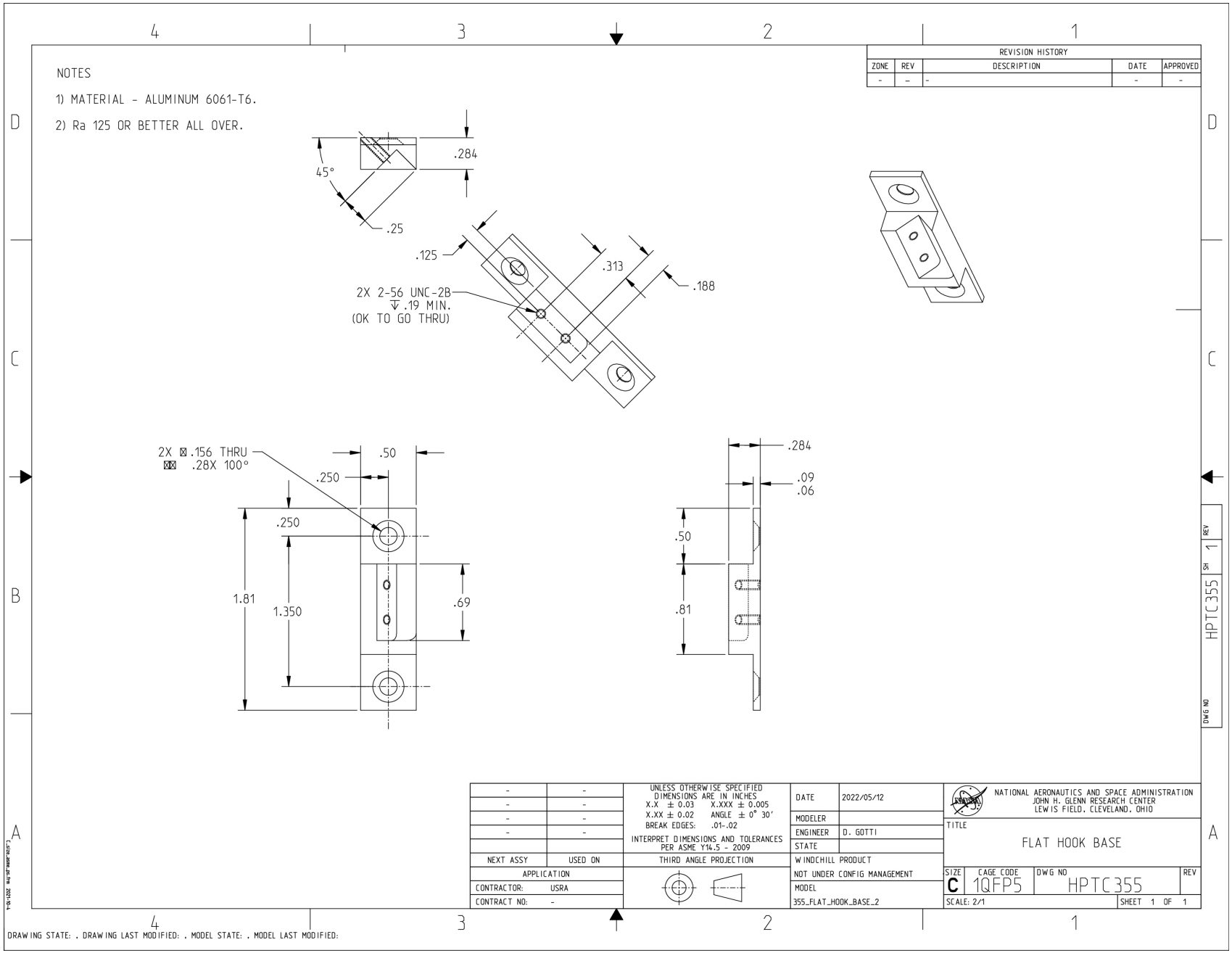

Figure B.12.—Fiber hook base.

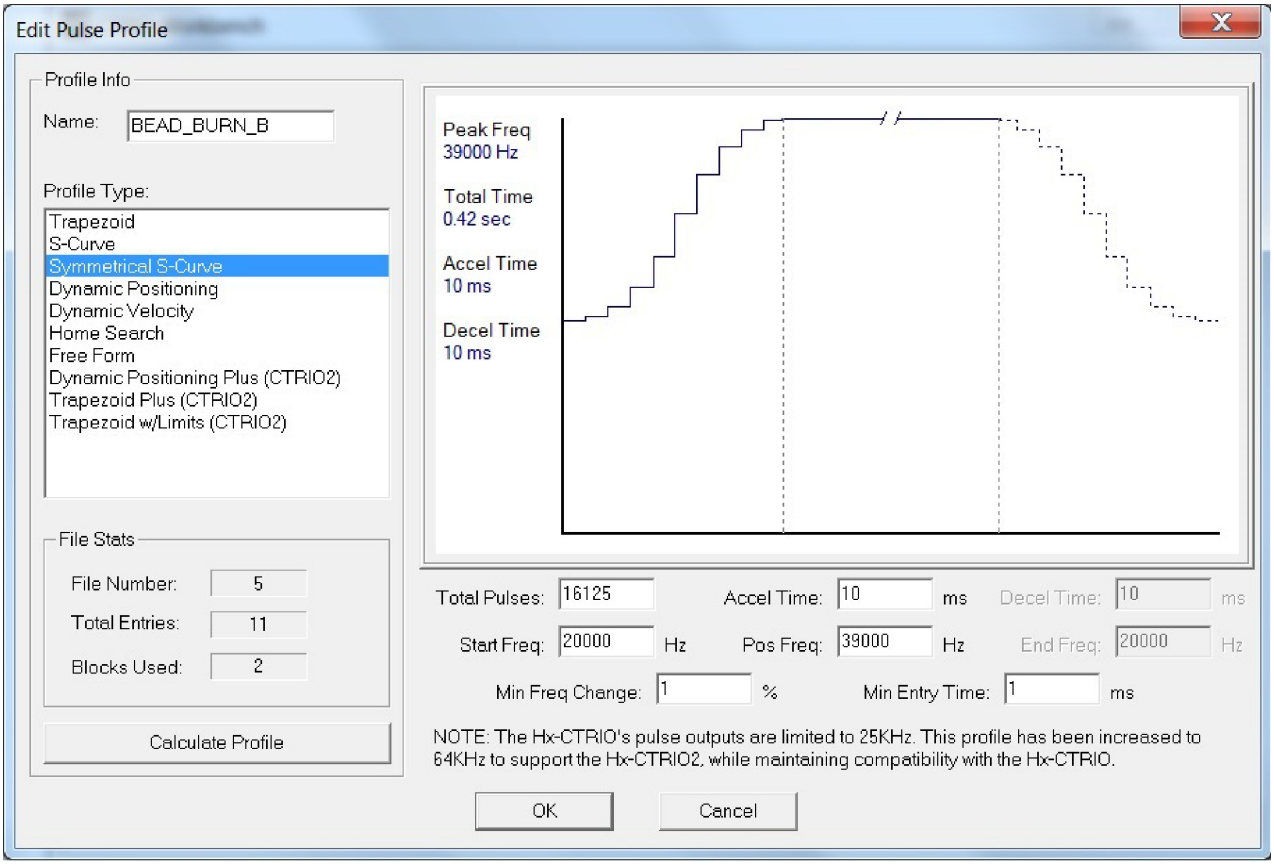

Figure B.13.—Droplet insertion profile.

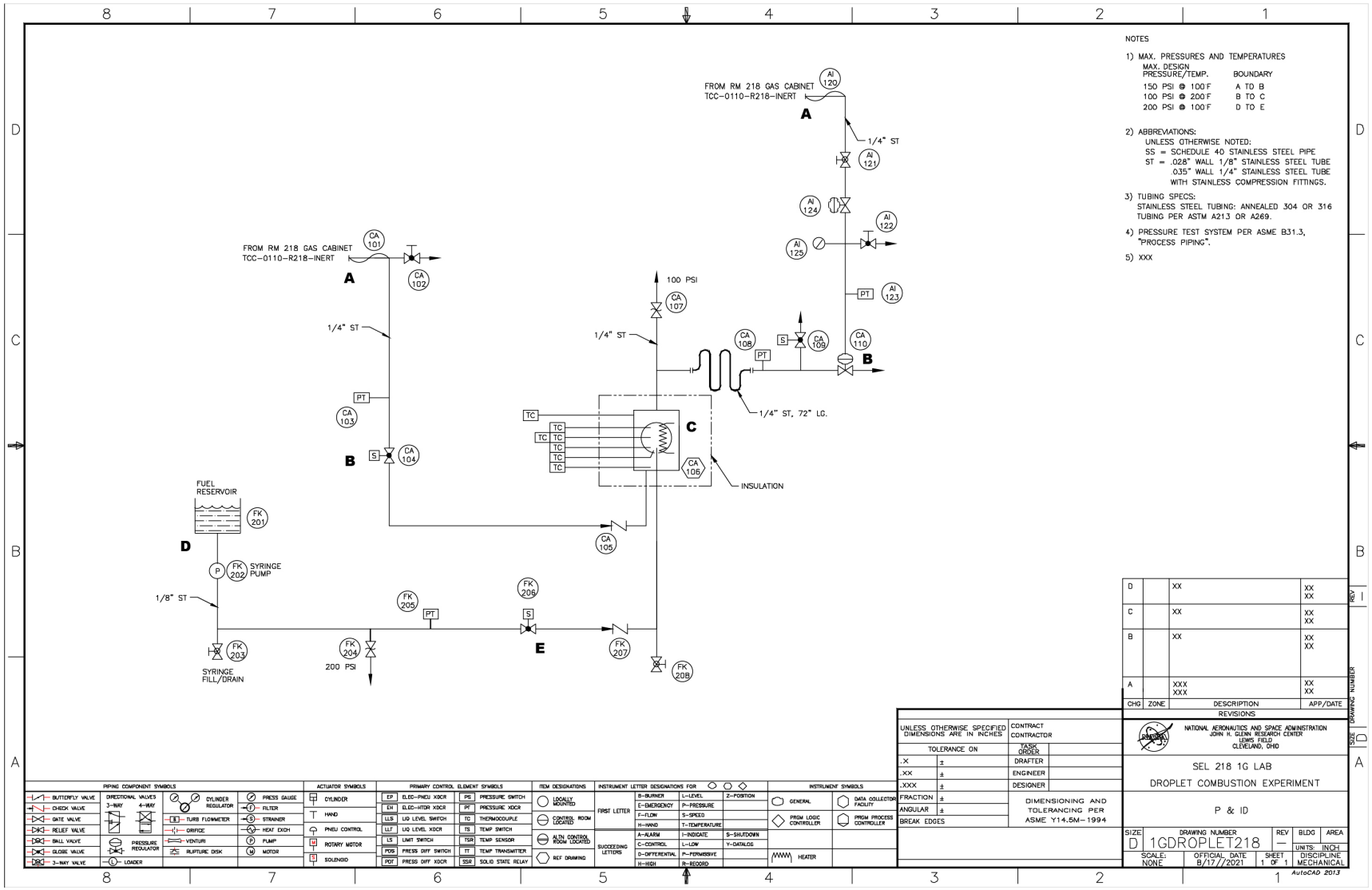

Figure B.14.—Droplet combustion experiment plumbing.

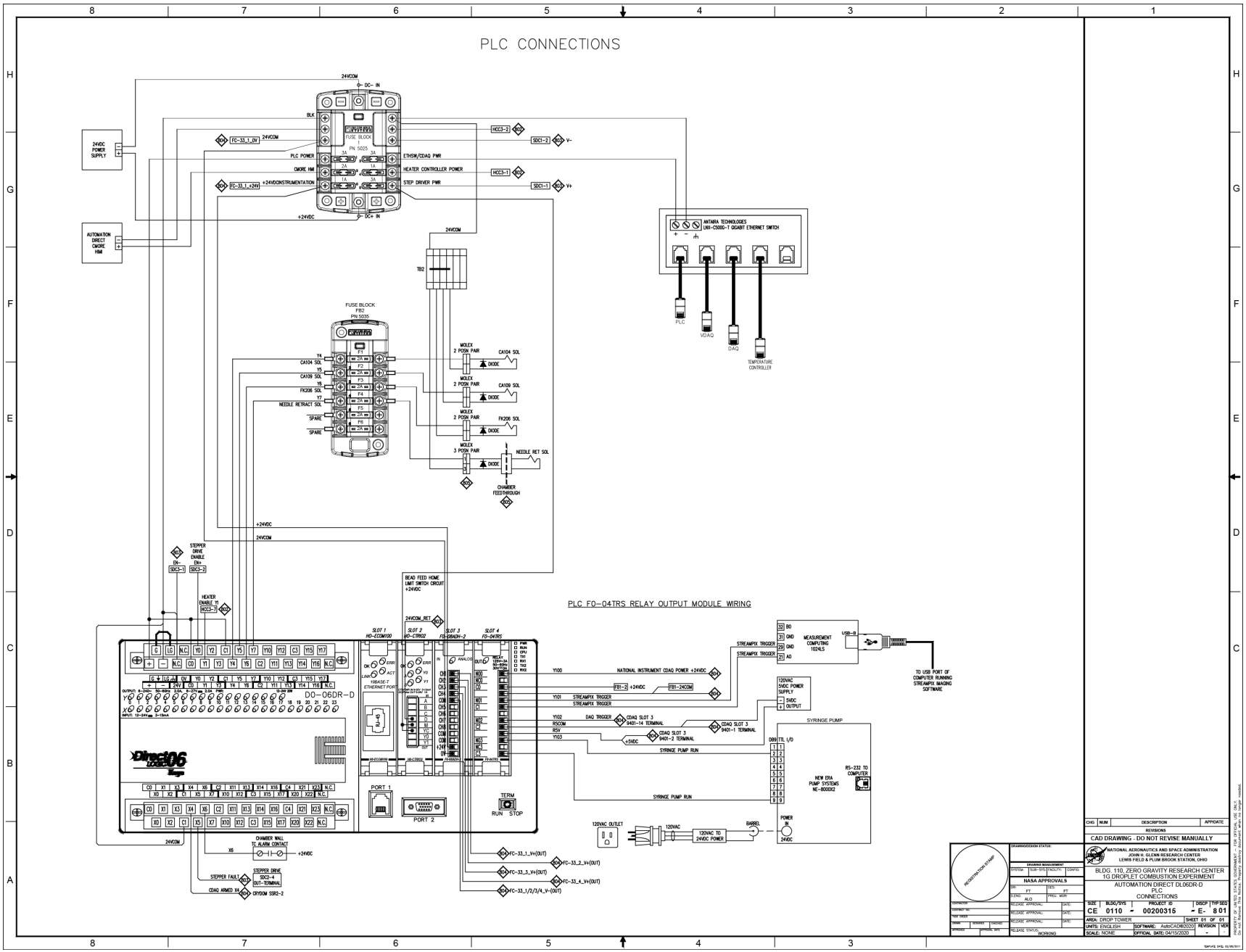

Figure B.15.—PLC connections.

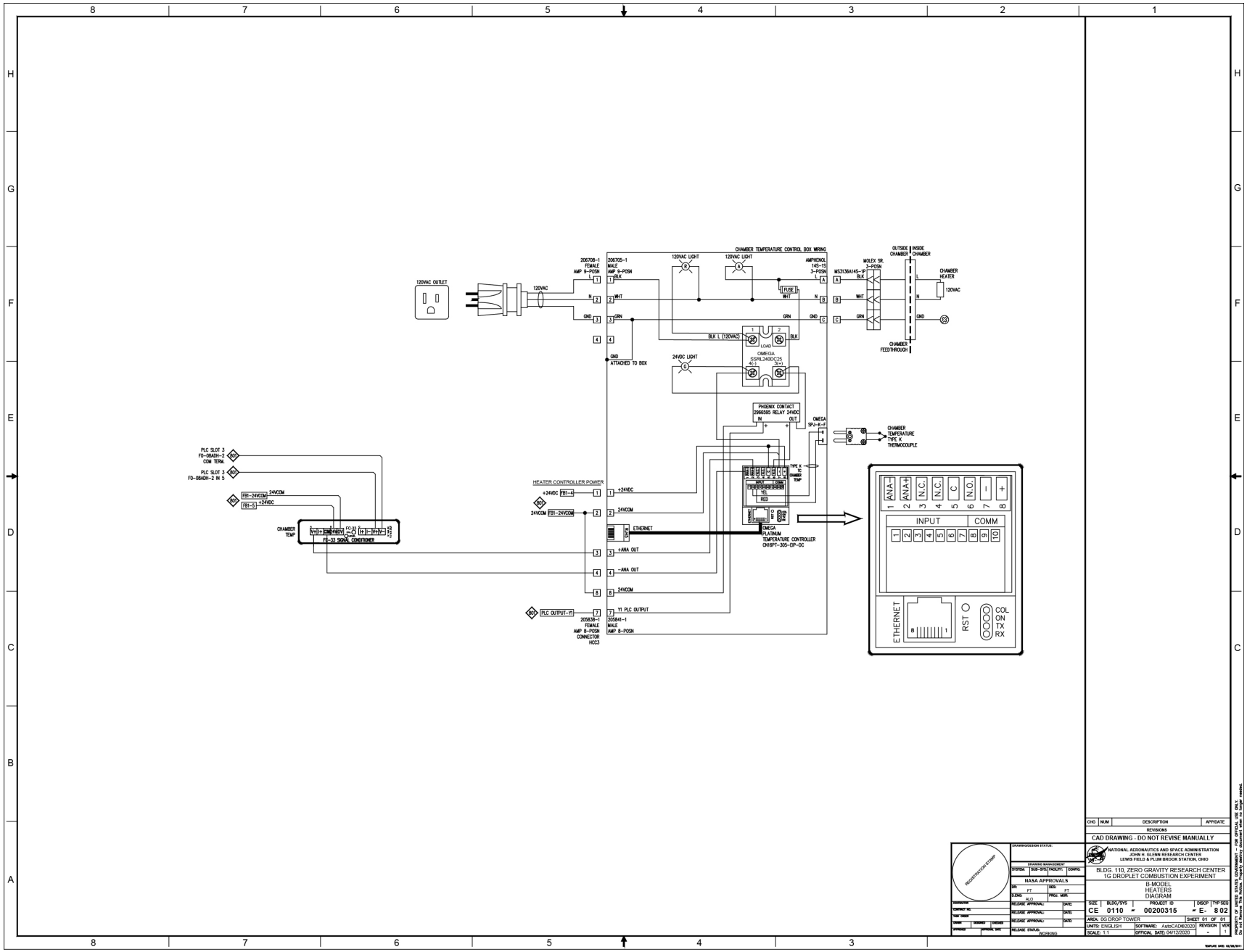

Figure B.16.—Temperature control box connections.

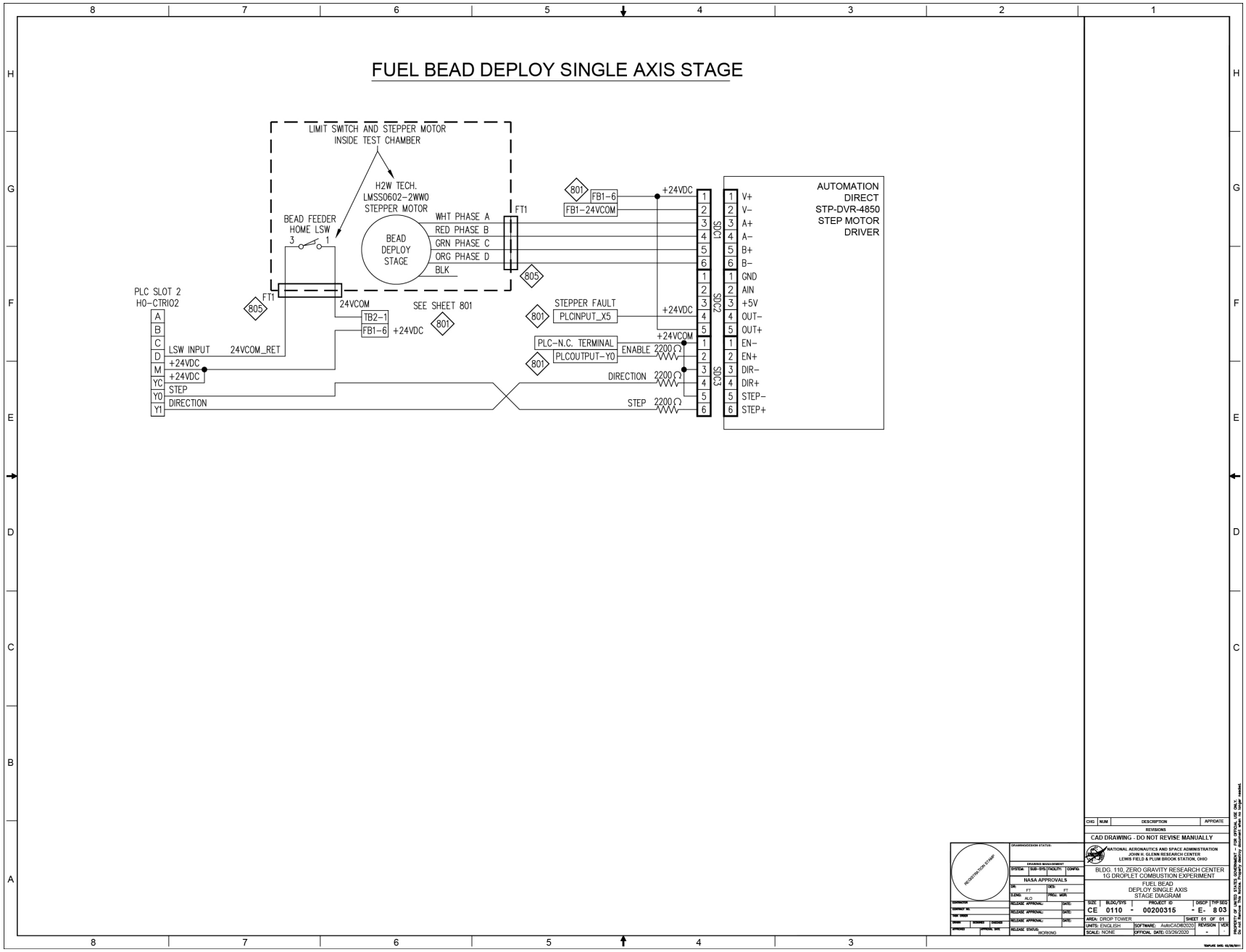

Figure B.17.—Droplet deployment connections.

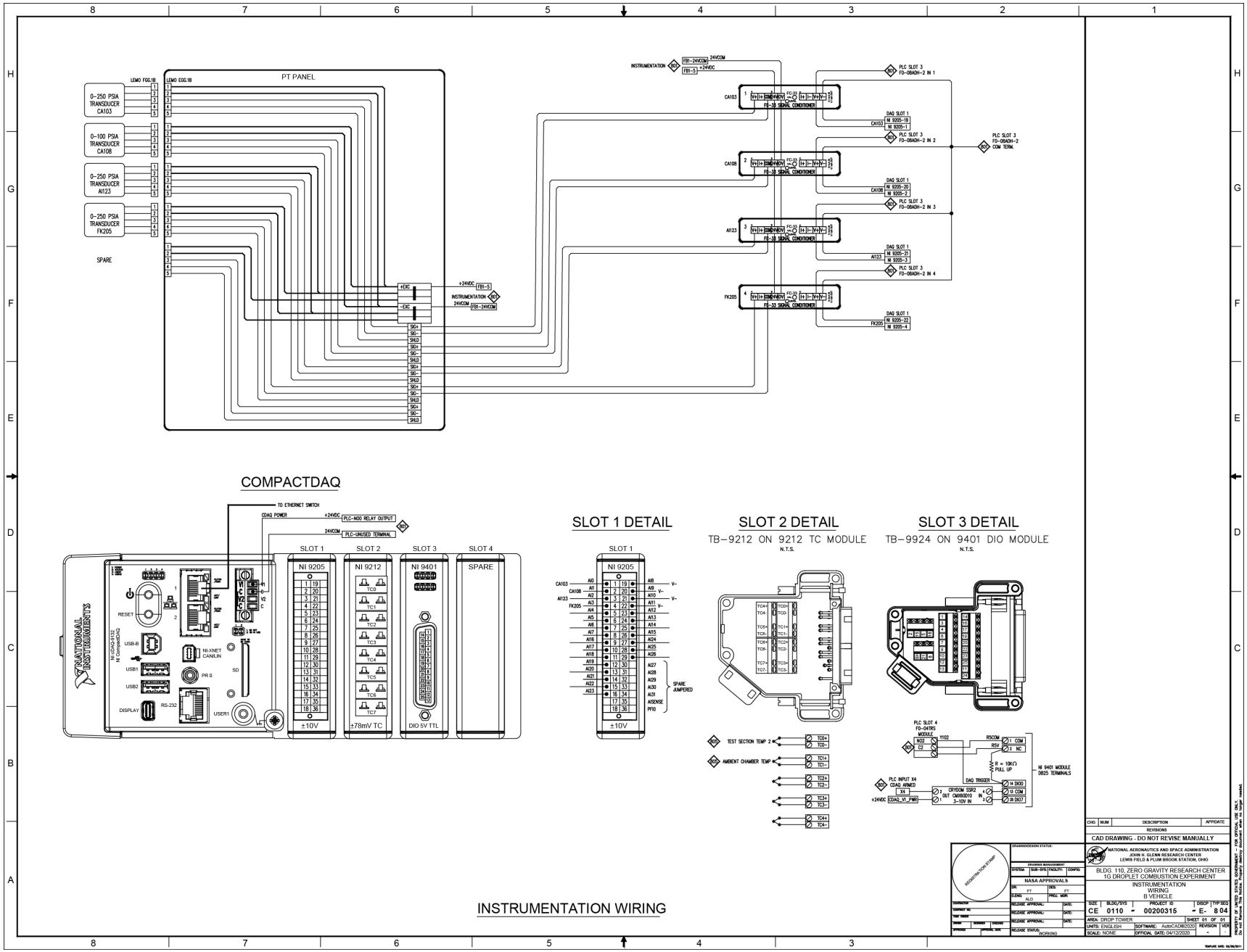

Figure B.18.—Compact data acquisition connections.

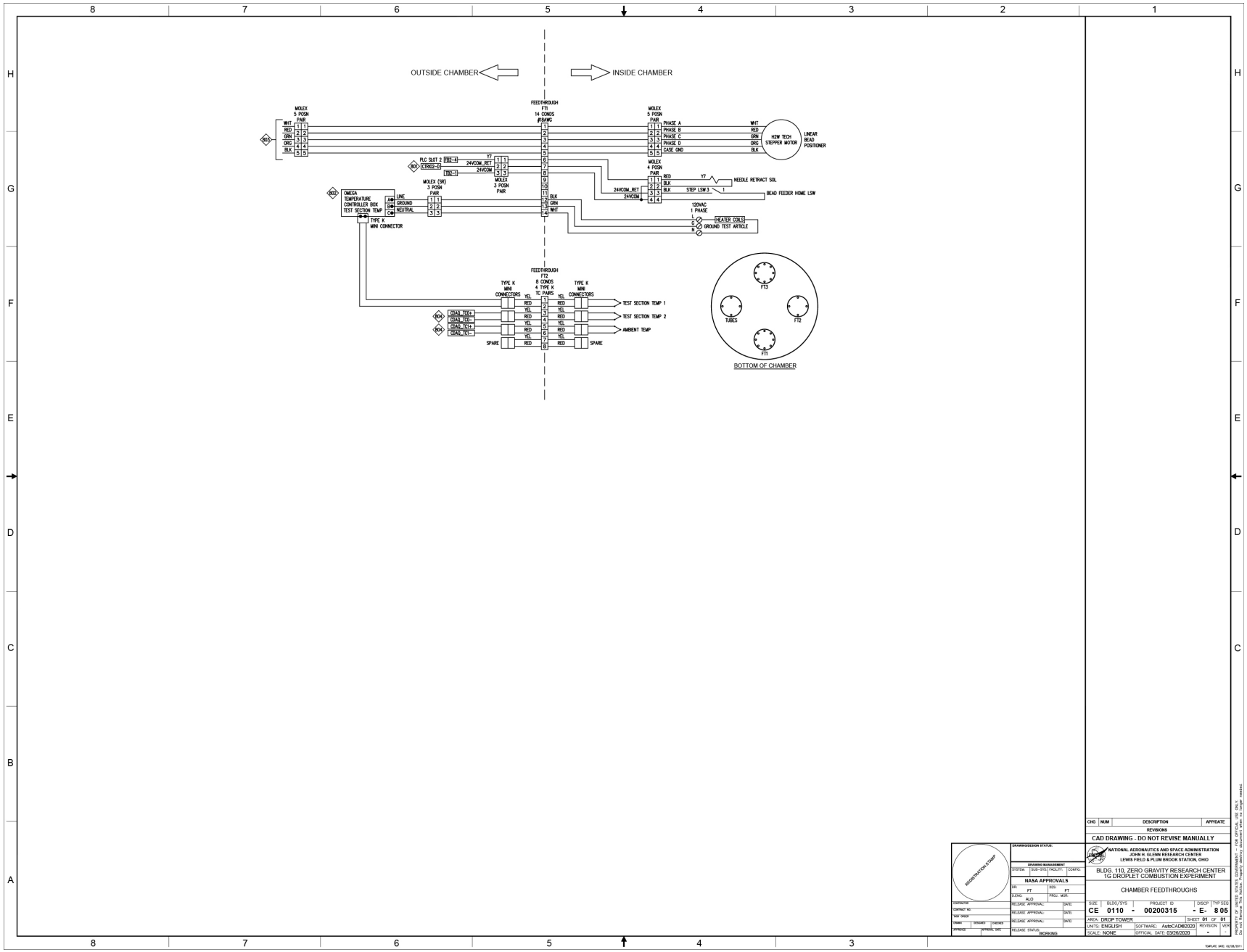

Figure B.19.—Chamber feedthrough connections.

TABLE B.1.—DROPLET COMBUSTION EXPERIMENT PARTS LIST

Part no.	Model no.	Size	Material	Rating	Description
CA 101	Swagelok SS4BHT36	6.35-mm (1/4-in.) tube	Polytetrafluoroethylene (PTFE) lining, stainless steel (SS) braid	204 atm (3,000 psia) 294 K (70 °F)	0.9-m- (3-ft-) long flex hose
CA 102	Swagelok SS1KS4	6.35-mm (1/4-in.) tube	SS body, polychlorotrifluoroethylene (PCTFE) seat	340 atm (5,000 psia) 311 K (100 °F)	Manual globe valve
CA 103	Setra 204	6.35-mm (1/4-in.) NPTF[1]	SS	10.2 atm (150 psia) 353 K (175 °F)	Pressure transducer
CA 104	Peter Paul H22M7DGM	3.175-mm (1/8-in.) NPT[2]	SS body, PCTFE seat	340 atm (5,000 psia) 339 K (150 °F)	Solenoid valve $c_v = 0.01$
CA 105	Swagelok SSCHS41	6.35-mm (1/4-in.) tube	SS body, fluorine kautschuk material (FKM) seat	408 atm (6,000 psia) 311 K (100 °F)	Spring check valve $c_v = 0.67$
CA 106	NASA	Multi	6061-T6	7.74 atm (113.8 psia) 366 K (200 °F)	Pressure vessel
CA 107	Kunkle 0542A01AKM0110	6.35-mm (1/4-in.) NPT[2]	Brass body, FKM seat	13.6 atm (200 psia) 422 K (300 °F)	Relief valve
CA 108	Setra 204	6.35-mm (1/4-in.) NPTF[1]	SS	6.8 atm (100 psia) 353 K (175 °F)	Pressure transducer
CA 109	Peter Paul H22M7DGM	3.175-mm (1/8-in.) NPT[2]	SS body, PCTF seat	340 atm (5,000 psia) 339 K (150 °F)	Solenoid valve $c_v = 0.01$
CA 110	Equilibar LF1SNN12BNSMP 500T150G10VVB	3.175-mm (1/8-in.) NPT[2]	SS body, FKM seat, PTFE/glass diaphragm	34.0 atm (500 psia) 422 K (300 °F)	Back pressure regulator $c_v = 0.07$
AI 120	Swagelok SS4BHT36	6.35-mm (1/4-in.) tube	PTFE body, SS braid	204 atm (3,000 psia) 297 K (75 °F)	0.9-m (3-ft) long flex hose
AI 121	Swagelok SS–43S4	6.35-mm (1/4-in.) tube	SS ball and body, PTFE seat	204 atm (3,000 psia) 311 K (100 °F)	Ball valve $c_v = 1.4$
AI 122	Swagelok SS–1KS4	6.35-mm (1/4-in.) tube	SS body, PCTFE seat	340 atm (5,000 psia) 311 K (100 °F)	Globe valve $c_v = 0.37$
AI 123	Setra 205–2	6.35-mm (1/4-in.) NPTF[1]	SS	17.0 atm (250 psia) 353 K (175 °F)	Pressure transducer
AI 124	Brooks Instrument 8601D	3.175-mm (1/8-in.) NPT[2]	Aluminum body, nitrile rubber seat	17.0 atm (250 psia) 333 K (140 °F)	Pressure regulator
AI 125	Winters P9U901408U	3.175-mm (1/8-in.) NPT[2]	Brass	10.9 atm (160 psia) 339 K (150 °F)	Pressure gauge
FK 201	KDS Scientific 780807	3.175-mm (1/8-in.) tube	SS body, perfluoroelastomer (FFKM) seat	102 atm (1,500 psia) 311 K (100 °F)	Syringe
FK 202	New Era NE–8000X2	Multi	Multi		Syringe pump
FK 203	Swagelok SS–41S2	3.175-mm (1/8-in.) tube	SS ball and body, PTFE seat	170 atm (2,500 psia) 311 K (100 °F)	Ball valve $c_v = 0.2$
FK 204	Swagelok SS–RL3S4	6.35-mm (1/4-in.) tube	SS body, FKM	20.4 atm (300 psia) 294 K (70 °F)	Spring relief valve
FK 205	Setra 205–2	6.35-mm (1/4-in.) NPTF[1]	SS	17.0 atm (250 psia) 353 K (175 °F)	Pressure transducer
FK 206	Peter Paul H22M7DGM	3.175-mm (1/8-in.) NPT[2]	SS body, PCTFE seat	340 atm (5,000 psia) 339 K (150 °F)	Solenoid valve $c_v = 0.01$
FK 207	Swagelok SS–CHS2–1/3	3.175-mm (1/8-in.) NPT[2]	SS	408 atm (6,000 psia) 478 K (400 °F)	Check valve $c_v = 0.67$
FK 208	Swagelok SS–41S2	3.175-mm (1/8-in.) NPT[2]	SS ball and body, PTFE seat	170 atm (2,500 psia) 311 K (100 °F)	Ball valve $c_v = 0.2$

[1]National Pipe Thread Fuel.
[2]National Pipe Thread.